Analysis of the influence of device-scale wind field on the sampling efficiency of pollen as a representative bioaerosol

2020

Kenji MIKI

Contents

Chapter 3.
Comparative efficiency of airborne pollen concentration evaluation in two pollen sampler designs related to impaction and changes in internal wind speed

Chapter 4.
Evaluating inaccurate pollen concentration evaluation caused by turbulent vertical wind flux

List of figures

List of tables

Chapter 1

General introduction

1.1 Research branch of aerobiology

Aerobiology is an interdisciplinary branch of biology that focuses on airborne bioparticles including viruses, microorganisms, fungal spores, and pollen. The field was established in the 19th century when Louis Pasteur became the first to illustrate airborne microorganisms [Morris *et al*., 2011]. Since that time, aerobiological studies have expanded to determine which bioparticles exist in the atmosphere and to what extent.

1.1.1 Determination of bioaerosol dispersion range

Recent aerobiological studies have investigated the dispersion range of the biosphere. Smith *et al*. (2018), for example, sampled airborne microbial particles in the troposphere and the stratosphere, finding that the bacterial particles were distributed homogeneously under altitudes of 12 km. It was also observed that the atmospheric concentrations of some taxa, such as *Lachnospiraceae* and *Ruminococcaceae*, were higher within the troposphere. Further to this, studies by Bryan *et al*. (2019) found that some microorganisms are capable of surviving in the conditions of the lower stratosphere.

In addition to airborne bioaerosol samplings, *in situ* bioaerosol detections have been performed in the upper atmosphere, with Immler *et al*. (2005) finding that aerosols generated from the burning of biomass could be identified in the stratosphere by a lidar system using fluorescence detection methods.
Aerobiological studies have also been performed underground. Picco *et al*. (2000) investigated the airborne spora in two underground stations located in Milan, Italy. This underground sampling indicated to what extent the mycoflora of an indoor environment depends both on the fungal spora coming from outside and the capacity of the fungi to colonize the different indoor conditions.

1.1.2 Application of aerobiology

Aerobiology has primarily been applied to monitoring common bioaerosols of interest, attracting much interest from immunological researchers in relation to the control of microbial infections [Lackemeyer *et al*. 2014; Fernandez *et al*. 2019; King *et al*. 2013; Phillpotts *et al*. 2010; Olmsted 2008].

Aerobiological studies have also been applied to the monitoring of airborne allergic pollen. Conventionally, airborne pollen concentrations are considered an indicator of the allergy risk to those allergic to pollen [Frenz 2001]. As an example, datasets from pollen traps have been used to evaluate the health impacts of ragweed in Lyon, France, where it exists as a common wind-pollinated plant [Thibaudon *et al*. 2009]. Airborne pollen concentration datasets have also been utilized to evaluate the indoor and outdoor levels of cedar and cypress pollens at a kindergarten in Japan in order to study the influence of exposure to these allergenic pollens during infancy [Yamamoto *et al*. 2010]. According to a report by the World Allergy Organization (WAO), the proportion of those allergic to pollen is estimated to be in the range of 10% to 40% of the population of the country in question [Pawankar *et al*. 2011]. In order to minimize serious impacts of pollen on human health, accurate pollen data is required to provide precise predictions of the spatial and temporal distributions of pollen, thus allowing affected patients to minimize their exposure to pollen. Understanding spatiotemporal patterns of allergen dispersal is important for mitigating impacts on people who are allergic to pollen or fungal spores. Pollen dispersal has been investigated via global-scale networks [Buters *et al*. (2018); Ritenberga *et al*. (2018)], and many studies have investigated allergen dispersal from an aerobiological perspective [e.g., Favero-Longo *et al*. (2014); Jedryczka *et al*. (2015); West and Kimber (2015); Yli-Panula *et al*. (2009); Zhang *et al*. (2014)]. Aerobiological research has often aimed to understand the relationship between allergen dispersal and meteorological factors [e.g. Laaidi (2001); Rojo *et al*. (2015); Visez *et al*. (2015)].

As a result, establishing a method to evaluate airborne pollen concentrations is vital for the fields of immunology and aerobiology.

As previously discussed, pollen has been extensively studied for immunological purposes. However, fungal spores and pollen have also been a significant research interest in aerobiological studies in agricultural science. The primary purpose of studies on fungal spores has been the protection of plants and fruits to certain diseases [Aylor 1998; Frinking 1991; Hartill 1980; Blanco *et al*. 2004], while similar studies on pollen have been performed to either control the gene flow [Jarosz *et al*. 2003; Fernández-Rodríguez *et al*. 2014; Fernández-Llamanzares *et al*. 2014], or to understand phenological changes in vegetation [Estrella *et al*. 2006; García-Mozo *et al*. 2016; Jochner *et al*. 2012; Velasco-Jiménez *et al*. 2017]. Pollen grains from around the world have been sampled for these aerobiological studies.

In summary, aerobiological studies tend to focus on searching for microorganisms in extreme environments, the diffusion and transportation control of pathogens, and the observation of airborne pollen or fungal spores that deliver allergens or genetic information. This paper focuses on pollen as the representative bioaerosol of study.

1.2 Evaluation of airborne bioaerosol (pollen) concentrations

The aerobiological study has been based on the experimentally evaluated airborne bioaerosol concentrations, therefore selection of the appropriate sampling method is vital.

1.2.1 Gravitational samplers

Gravitational methods are designed to evaluate pollen deposition. The Durham sampler is one of the most commonly used gravitational samplers, consisting of two flat plates and a pole. The sampling plate is placed between the two flat plates, allowing it to sample deposited bioaerosol particles. The pollen concentration is determined by counting the number of deposited pollen grains on the sampling plate by visual observation. The Durham sampler is widely used in Turkey [Erkan *et al*. 2011], Japan [Yasaka *et al*. 2009; Lu *et al*. 2015], and Italy [Bricchi *et al*. 2000].

The Tauber trap is also a regularly utilized gravitational sampler, often used to sample palynological particles deposited on the ground. This method is widely used in China [Li *et al*. 2018], Poland [Deptula *et al*. 2018], Russia [Volkova and Severova 2017], Nigeria [Ezike *et al*. 2016], Latvia, Czech Republic, Switzerland, Greece, Bulgaria, Georgia, and the UK [Giesecke *et al*. 2010]

1.2.2 Volumetric samplers

Volumetric samplers are designed to evaluate the airborne concentrations of particles. Volumetric methods determine the atmospheric particle concentration by dividing the number of counted pollen grains by the volume of the sampled air as:

$$concentration = \frac{number\ of\ particles}{volume\ of\ the\ air}$$

The most widely used volumetric sampling method is the Hirst sampler. This sampler is designed to sample from the upwind, facing toward the flow of air. The sampling rate of the Hirst sampler is generally set at 10 L min^{-1}. The sampled air is blown onto sticky tape inside the sampler, impacting the particles in the air onto the tape. The sampled bioaerosols are counted and sorted by visual observation. The Hirst sampler has been used by Ríos *et al*. (2016), Hussain *et al*. (2014), and Peternel *et al*. (2006) for airborne pollen concentration evaluation.

Volumetric methods are considered preferable to gravitational methods in understanding the actual impact of pollen to human health because of the their proximation to the aspiratory mechanism [Cornell *et al*. 1961].

Various other volumetric methods, such as the Cascade impactor [Prado *et al*. 2015; Hassan and Lau 2011; Taylor *et al*. 2002; Riediker *et al*. 2000], designed to sample filters inside the sampler, the Coriolis sampler [Gomez-Domenech *et al*. 2010; Carvalho et al. 2008], designed to sample using rotating liquid, or the Air-o-cell [Michel *et al*. 2012], which samples particles impacting onto a sampling plate, have also been used to determine airborne pollen concentration. In order to evaluate the impact that pollen has on human health, personal pollen counters have also been developed. Adhikari *et al*. (2003), studied the Button Personal Inhalable Aerosol Sampler, which is a portable volumetric sampler. This instrument was observed to be efficient for personal sampling of outdoor aeroallergens.

1.2.3 Development of automatic pollen counters

Improvements in the field of volumetric methods have also led to the development of automatic pollen counters. Some counters evaluate the light scattering patterns of pollen gains [Kawashima *et al*. 2007; Surbek *et al*. 2011; Crouzy *et al*. 2016], while some use the relationship between scattering intensity and the blue-to-red fluorescence ratio [Mitsumoto *et al*. 2010]. Others use fluorescence [O'Conner *et al*. 2015], artificial neural networks [Šauliene *et al*. 2019], or light scattering patterns and polarization [Delaunay *et al*. 2007]. These automatic pollen counters have been developed to realize fast and/or real-time identification with the benefit of low labor.

Through the application of these automatic pollen counters, nationwide-scale pollen concentration monitoring networks have been established. There are currently 879 active automated pollen monitoring stations worldwide, including two stations on the American continent and 120 stations in Japan [Buters *et al*. 2018].

Further developments in automatic pollen counters have been made using the datasets provided from these large-scale pollen monitoring systems. Takahashi *et al*. (2018) suggested that the pollen concentration data from automatic pollen counters set up at 14 sampling points in northern Japan illustrated that weather fronts brought in significant quantities of pollen grains. Brennan *et al*. (2019) observed that allergen concentrations in the atmosphere change substantially with the changes in the grass pollen season, again by automatically monitoring the nation-wide automatic pollen sampling system.

Worldwide automatic pollen monitoring networks have also been established by theoretically setting the number and position of representative monitoring points using clustering analysis [Oteros *et al*. 2019].

1.3 Comparison of sampling efficiencies

Although various methods have been invented and developed in order to determine the atmospheric pollen concentration, it is difficult to know if these samplers provide the actual atmospheric pollen concentration. In order to determine which method or sampler is the most effective in determining the actual airborne pollen concentration, various researchers have compared the pollen sampling efficiencies of different types of samplers.

1.3.1 Volumetric samplers vs. Volumetric samplers

Mehta *et al*. (1996) found that the SAS Super 90 and RCS plus pollen samplers, both handheld portable volumetric particle samplers, are significantly less efficient than the Andersen or Hirst Traps. Through comparison of the SKC total dust sampler, which was designed to measure personal exposure to pollen, and the Hirst sampler, placed at various monitoring stations, Riediker *et al*. (2000) found that, while the atmospheric pollen concentration data obtained at monitoring stations was useful in determining personal exposure to pollen, the personal sampler only observed approximately 30% of the airborne pollen detected by the Hirst sampler.

The Cour pollen trap, which was designed to filter airborne particles and consists of a vertical gauze filter impregnated with silicone oil, has been shown to be capable of capturing a wider range of pollen types than the Hirst sampler [Tomás *et al*. 1997].

Previous works have also evaluated the efficiency of the Hirst sampler compared to the Air-o-Cell, with Michel *et al*. (2012) concluding that the Air-o-Cell exhibited equal performance when compared to the Hirst method.

Personal volumetric pollen samplers have also been studied in contrast with stationary samplers. An experiment performed by Fiorina (1997) indicated that a personal pollen sampler (Partrap FA52, Coppa, Biella, Italy) was capable of sampling at essentially the same efficiency as the Hirst sampler, regardless of the pollen type.

1.3.2 Gravitational samplers vs. Volumetric samplers

Volumetric samplers are important to aid understanding of the actual airborne particle concentration. On the other hand, gravitational samplers are commonly used due of their simplicity. In a study by Serrano-Silva *et al*. (2018), the Durham sampler, which is the most representative gravitational sampler, and the Hirst sampler were compared. The authors concluded that the Hirst sampler samples the largest amount of airborne bacterial diversity. Another investigation involving the Durham and Hirst samplers indicates that both setups shows comparable sampling results [Crispen *et al*. 2010].

With regard to further sampling comparisons, the Hirst sampler and the Tauber Trap were also evaluated to find that they exhibit approximately the same efficiencies [Levetin *et al*. 2000]. Volkova and Severova (2017) also concluded that both the Hirst sampler and the Tauber Trap show similar pollen spectra.

Furthermore, through comparison of the Personal Aeroallergen Sampler, which is a personal passive sampler for airborne particle, and the Durham sampler, Yamamoto *et al*. (2007) suggested that personal samplers do not always successfully detect the pollen levels at the peak of the season.

Bhat and Rajasab (1989) also investigated the relationship between particle size and monitoring efficiency, suggesting that, in comparison with the Hirst trap, the Vertical Cylinder Spore Trap, which was a wind-vane non-volumetric impaction sampler, exhibited better efficiencies in cases where the particles were less than 20 μm in size. However, when the monitoring efficiencies were defined as the number of pollen grains in a given volume, the cylinder trap was found to be less efficient than the Hirst.

1.3.3 Other comparisons

Other sampling methods exist that are not classed as volumetric or gravitational methods. For example, a comparison between the Durham sampler and the Rotorod sampler, which is designed to sample airborne particles using rods, implied that these two methods display similar pollen trends with high correlation [Sun *et al*. 2017]. Furthermore, a comparison of pollen counts by the Burkard 7-day spore trap, the Burkard Personal Air sampler, and the Rotorod sampler suggested significant differences in terms of the concentrations sampled of Urticaceae and Poaceae pollen [Peel *et al*. 2014]. While the Hirst sampler was superior to the Rotorod trap in detecting small pollens such as Urticaceae [Crisp *et al*. 2013], Heffer *et al*.

(2005) indicated that the measurement efficiencies of the Rotorod, the Air-o-Cell, and a 37-mm open-faced filter cassette were at almost equivalent, but that the Hirst sampler showed pollen counts 1.6 times larger than the other samplers. Frenz (1999) suggested that the Hirst sampler is more efficient for capturing pollens whose radii were smaller than 10 μm, while the Rotorod is more efficient for the sampling of larger particles.

1.4 Objectives

Previous research on the sampling efficiencies of the various pollen methods aforementioned have focused on simple comparisons of the numbers of sampled pollen grains.

These studies, however, did not analyze what causes the discrepancies in the pollen sampling efficiencies among the different sampling methods. Therefore, in this paper, two different types of sampler have been compared in each chapter, with the causes of the discrepancies in sampling efficiencies explained in terms of aerosol physics, probability and fluid dynamics.

By revealing the relationship between the physical characteristics and sampling efficiencies, airborne pollen concentration data from various devices will be comparable with each other, meaning that the global-scale monitoring and reliable determination of airborne pollen concentrations can be realized.

In Chapter 2, the sampling efficiency of a Hirst-style inlet, which is designed to sample airborne pollen grains from the wind direction, and the conical inlet, which samples the deposited pollen grains, have been compared. From the discrepancies in the sampling efficiencies, the relationship between wind direction, wind speed and sampling efficiency have been evaluated.

In Chapter 3, the pollen sampling efficiencies of the two-layered style inlet, the most-often used inlet in Europe, and that of the Hirst-style inlet have been compared. These two-layered inlets are designed to cancel the wind speed, therefore the influence that the wind has on pollen sampling was analyzed from a mechanical viewpoint. This was achieved by comparing the Hirst-style inlet sampling pollen grains with the wind direction and the two-layered sampling inlet.

In Chapter 4, the pollen sampling efficiency of the gravitational method (the Durham sampler) and the volumetric (the Hirst sampler) method have been compared. This was carried out by theoretically calculating the airborne pollen concentration from the pollen deposition data evaluated using the gravitational method.

Chapter 5 includes the summary as well as general discussion.

Chapter 2

Effect of device-scale wind on measurement of airborne pollen concentrations using volumetric methods

2.1 Introduction

Various methods have been developed for accurate evaluation of airborne pollen concentrations [Mullins and Emberlin 1997], which are conventionally evaluated through various types of pollen traps [Thibaudon *et al*. 2013].

Some scientists have worked on evaluating the efficiencies of various types of inlets attached to volumetric-type samplers. A previous study suggested that bioaerosol counts vary depending on the direction of the orifice of the inlets [Willeke *et al*. 1992; Michel *et al*. 2012]. Grinshpun *et al*. (1994) mathematically evaluated efficiencies of various inlets by measuring their physical characteristics. Davies (1968) suggested that a relationship exists between aerosol sampling efficiency and the direction of the inlet device.

The studies mentioned above were carried out to seek the best method for evaluating airborne pollen concentrations. However, the accuracies of airborne pollen traps are strongly influenced by meteorological elements. A previous study suggested that considering precipitation might help predict future pollen concentrations [Galan *et al*. 2000]. Another study on the relationship between meteorological conditions and airborne pollen concentrations implied that airborne pollen concentrations were significantly influenced by humidity and temperature with small p values ($p < 0.05$) [Veriankaite *et al*., 2011]. Analyzing 15-year meteorological datasets and airborne pollen concentrations, Gioulekas *et al*. (2004) also found that mean temperature was one of the important meteorological conditions that strongly influences airborne pollen concentrations (r = 0.43, $p < 0.05$). Kasprzyk *et al*. (2014) also suggested that temperature and precipitation were important indicators of airborne pollen concentrations in Poland, and Toth *et al*. (2011) found the same trend for Zagreb, Croatia. Additionally, previous studies demonstrated the influence of wind on the transport of pollen grains depending on the characteristics of the experimental site [Hamada *et al*. 2015; Santos *et al*. 2005]. High pollen concentrations were detected when changes in wind velocity were approximately 1–2 m s^{-1} [Sauliene and Veriankaite 2012]. Kizilpinar *et al*. (2011) suggested that airborne pollen concentrations are influenced by daily temperature (r = 0.16, $p < 0.001$ for tree; r = 0.28, $p < 0.001$ for grass; r = 0.32, $p < 0.001$ for weed), wind velocity (r = 0.17, $p < 0.001$ for grass; r = 0.15, $p < 0.002$ for weed), and hours of sunshine (r = 0.14, $p < 0.001$ for tree; r = 0.25, $p < 0.001$ for grass; r = 0.21, $p < 0.001$ for weed).

Some studies have shown that meteorological conditions might lead to inaccurate pollen concentration data. Research conducted by Latorre *et al*. (2008) revealed that, in combination with some meteorological conditions such as wind speed or relative humidity, the difference in the capturing mechanisms of pollen traps might cause an inaccuracy in pollen concentration data. Gagnon and Comtois (1992) also suggested that meteorological conditions might have an influence on the efficiencies of the Durham and Rotorod traps. Thus, in order to detect the influences of meteorological factors on pollen concentrations, meteorological observations were performed in this study. In addition, because previous studies suggested that changes in wind path or direction might lead to changes in particle dispersion processes [e.g., Gupta *et al*. 2012, Mavroidis *et al*. 2007], and in order to evaluate the effect of the physical characteristics of rooftops on pollen counts, an experiment to evaluate the wind path around an obstacle was carried out.

This chapter seeks to evaluate the scale of the differences of pollen counts captured by different types of volumetric-type samplers in relationship to meteorological conditions. In this experiment, pollen concentrations were evaluated using two different types of inlets into the pollen monitors: a funnel-type inlet and a wind vane intake. This was done to examine the difference between the efficiencies of vertically oriented inlets and that of horizontally oriented inlets caused by changes of micro-wind conditions on a rooftop.

2.2 Materials and methods

Two experiments were performed. One of the experiments was carried out to evaluate the aspiration efficiencies of two different inlets: a funnel inlet and a wind vane intake. The other experiment was performed in order to investigate the motion of wind blowing over an obstacle before reaching the pollen samplers.

2.2.1 Experiment at Payerne

To evaluate the aspiration efficiencies of the different inlet types, two automatic pollen monitors (KH-3000-01, YAMATRONICS, Japan) were used. The aspiration rates of the monitors were kept constant at 4.1 L min^{-1}. A conical glass funnel with a maximum diameter of 65 mm was installed as Monitor A, and a wind vane intake with side inlet was installed as Monitor B (**Fig. 2.1**). As shown in the figure, both the funnel inlet and the wind vane inlet were attached to the upper surfaces of each monitor, which was approximately 1.2 m from the surface of the rooftop. The two monitors were placed at the northeastern end of the rooftop of the two-story MeteoSwiss building (**Fig. 2.2**) in Payerne, Switzerland (46°48’48’’N, 6°56’35’’E, Altitude 490 masl). The study site was chosen because 1. various previous pollen monitoring experiments had been performed at the MeteoSwiss for their reliable pollen monitoring systems. 2. meteorological factors were simultaneously measured at the MeteoSwiss. At the experiment site, the pollen monitors were placed 1.0 m away from a wall whose height was also 1.0 m. Monitoring of daily and hourly average pollen concentrations using both monitors were carried out over 55 days from 8 April 2014 to 1 June 2014. In this experiment, the pollen count data reflect the total airborne pollen concentration. In order to convert the pollen counts into airborne pollen concentration, the pollen counts were multiplied by a coefficient, the collection factor, which was introduced to adapt the monitor counts to the Hirst counts [Kawashima *et al*. 2017]. The collection factor is the ratio of the total airborne pollen concentration evaluated by the Hirst sampler to the total airborne pollen counts by the pollen monitors during the experimental term. The collection factor was assumed to be 4.9 based on the Hirst counts at the experimental site for this experiment. For more details, the full outline of the pollen monitoring system is available in Kawashima *et al*. (2007). It should be noted that pollen concentrations evaluated by the pollen monitor are almost identical to the actual pollen concentrations in the atmosphere, and that, with the exception of the inlets, all parts of the devices consisted of the same components. Meteorological data for the experiment period were obtained from MeteoSwiss. Air temperature (°C), relative humidity (RH) (%), wind direction (degree), wind speed (m s^{-1}), precipitation (mm day^{-1}), and solar radiation (W

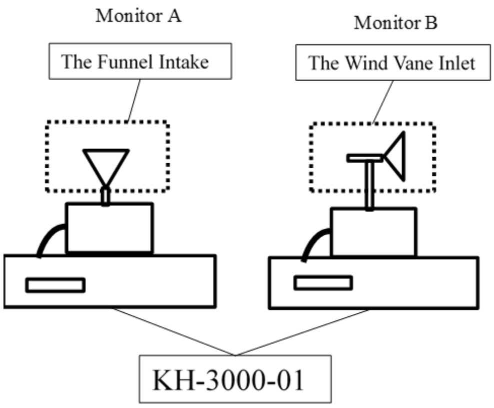

Fig. 2.1 Automatic pollen counters. A conical glass funnel inlet and a wind vane inlet are attached to KH-3000-01.

m^{-2}) were used in the analysis.

2.2.2 The micro-scale wind experiment

In order to evaluate the effect of an obstacle on upstream side of the wind path, horizontal and vertical wind speed around an obstacle were evaluated on the rooftop of the Kyoto

University Agricultural Science building (height = 20 magl, 35°1’N, 135°47’E) over a 40-day period between 30 November 2015 and 8 January 2016 (winter).

A Gill Propeller Anemometer (Model 27106) (Gill Instruments, Hampshire, UK) was connected to a Campbell CR10X data logger (Campbell Scientific, Logan UT, USA) 1.2 meters above the rooftop surface next to an obstacle to evaluate vertical wind flux (**Fig. 2.3a**). Data were recorded by the logger every hour. The Gill Propeller Anemometer was placed 1.0 m away from the obstacle (**Fig. 2.3b**). Horizontal wind direction and other meteorological parameters were recorded by a weather observation system (Onset Computer Corporation, Bourne, MA, USA), which was positioned close to the vertical anemometer. Another wind speed anemometer was set up approximately 1.0 m above the rooftop surface in order to evaluate horizontal wind speed.

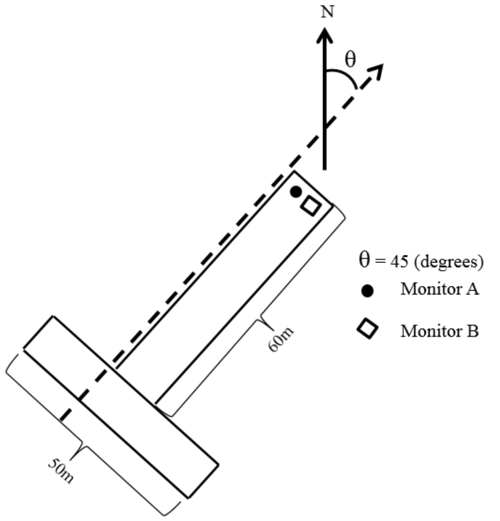

Fig. 2.2 Layout of the experimental devices on the MeteoSwiss building rooftop in Payerne

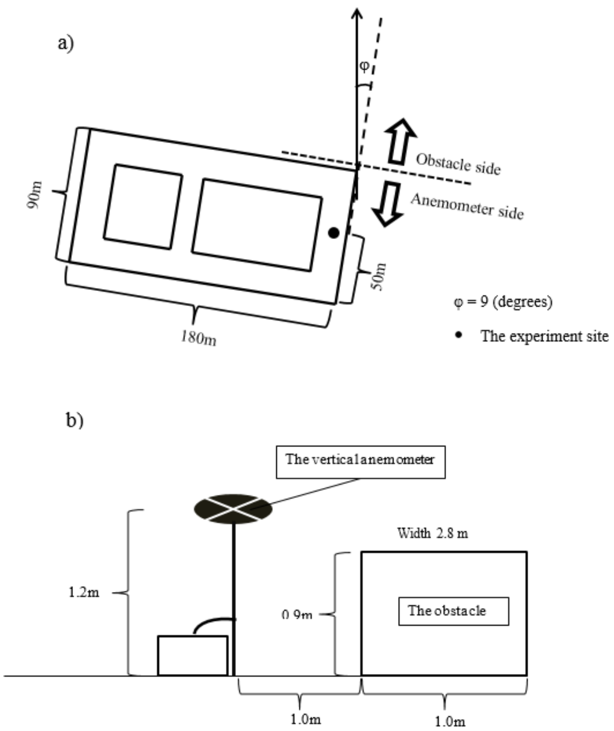

Fig. 2.3 Layout of the experimental devices on op of the Kyoto University Agricultural Science buildingin Kyoto. a) Location of the rooftop of the building: b) locations of the vertical anemometer and obstacle.

2.3 Results and discussion

2.3.1 Pollen concentrations

Fig. 2.4 shows daily changes in pollen concentrations recorded by Monitors A and B. Daily airborne pollen concentrations measured by both monitors show inconsistent trends, indicating inconsistencies in the efficiencies of both monitors. The correlation coefficient (r) of the pollen concentrations measured by Monitor A and Monitor B is 0.91. **Fig. 2.5** shows the circular histogram of pollen concentrations evaluated by Monitor A and B from each direction.

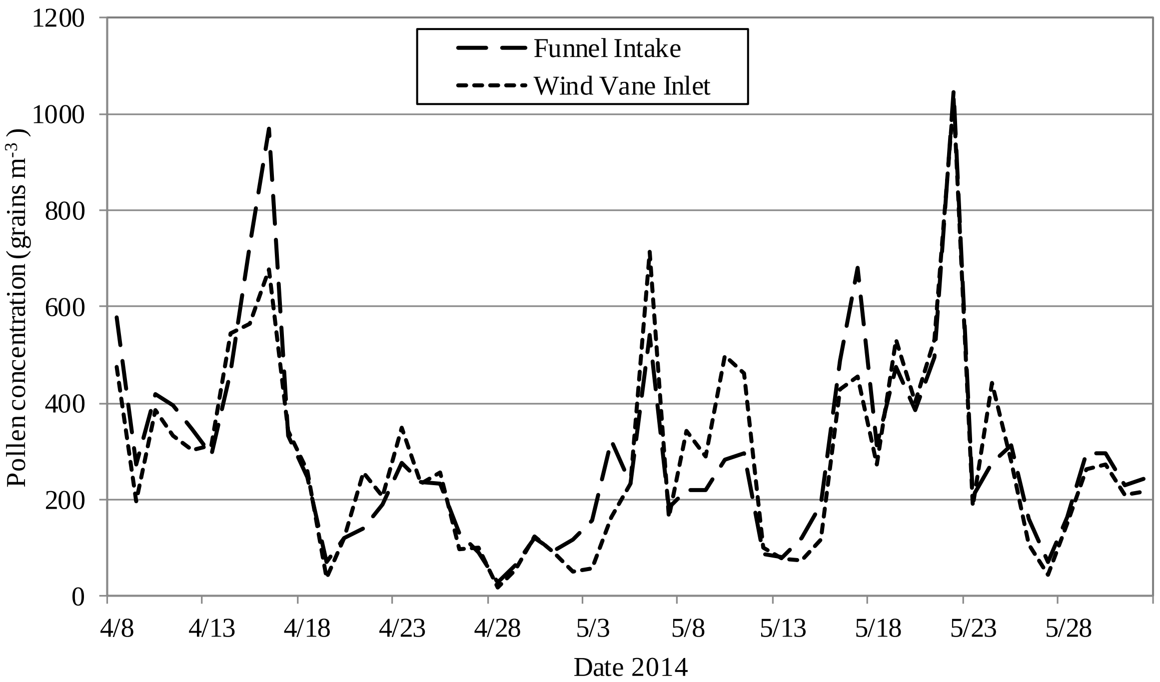

Fig. 2.4 Daily changes in pollen concentrations during the observation period.

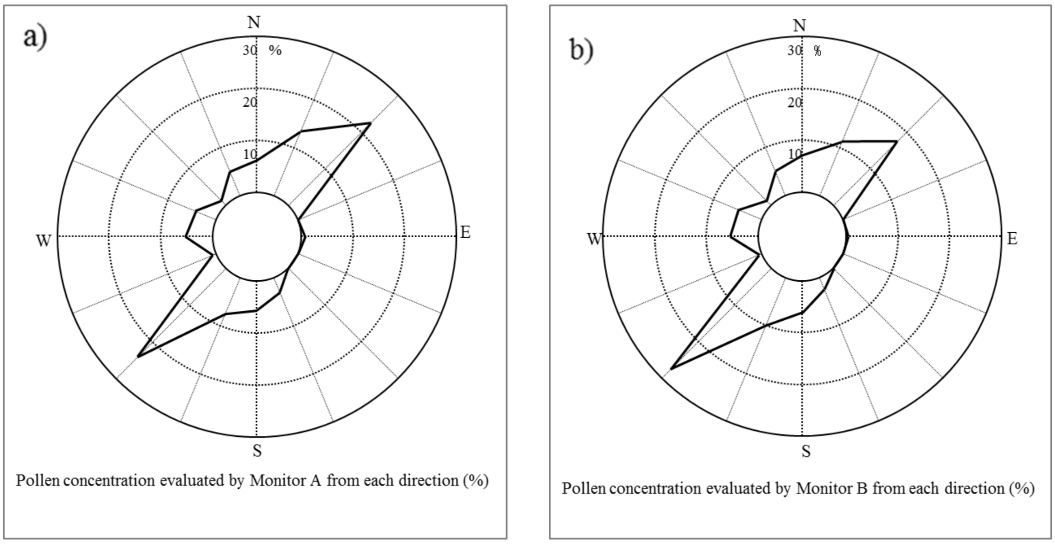

Fig. 2.5 Circular histograms of pollen concentrations from each direction evaluated by a) Monitor A; b) Monitor B.

Table 2.1
Correlation coefficients and p values between the pollen concentrations and meteorological factors.

Monitor A	Correlation coefficient (r)
Air temperture at 2m hight (degrees)	0.20
Relative humidity (%)	-0.64*
Wind speed (m s^{-1})	0.26
Solar radiation (W m^{-2})	0.37*
Precipitatio (mm day^{-1})	-0.15
*$p < 0.05$	

Monitor B	Correlation coefficient (r)
Air tempertur at 2m hight (degrees)	0.39*
Relative humidity (%)	-0.64*
Wind speed (m s^{-1})	0.21
Solar radiation (W m^{-2})	0.36*
Precipitation (mm day^{-1})	-0.15
*$p < 0.05$	

2.3.2 Relationship between airborne pollen concentrations and meteorological conditions

The relationship between meteorological conditions and airborne pollen concentrations was analyzed in this experiment in order to identify the dominant elements that affect pollen concentrations. Daily temperature, relative humidity, wind speed, wind direction, radiation, and precipitation were considered as the meteorological factors. The correlation coefficients and *p* values of the airborne pollen concentrations evaluated by Monitor A and Monitor B and meteorological factors are shown in Table 1. No significant relationships are shown between pollen concentrations and meteorological factors except relative humidity. **Fig. 2.6a** shows the relationship between airborne pollen concentrations evaluated by Monitor B and relative humidity (RH). The figure indicates that the pollen concentration decreases along with an increase in RH. The correlation coefficient (r) in the graph reaches -0.64, implying that the changes in the airborne pollen concentration strongly depend on relative humidity. In **Fig. 2.6b**, daily variations of relative humidity and pollen concentrations are represented. The figure also shows a strong correlation of relative humidity to the pollen concentrations.

2.3.3 Comparison of pollen concentrations using different types of inlets

The airborne pollen concentrations measured by the two pollen samplers with different inlet physical characteristics show different daily variations of pollen concentrations (**Fig. 2.4**). The airborne pollen concentrations evaluated by Monitor A and Monitor B from each direction is represented in **Fig. 2.5**. The figure indicates that the pollen grains mainly flew from the northeast and the southwest. A regression analysis was conducted, setting the difference between the pollen concentrations measured by Monitors A and B (DP; A − B (grains)) as the response variable, and wind direction as the explanatory variable (**Fig. 2.7**). The figure shows that the DP is positive when the wind direction is around 50 degrees and negative at a wind direction of around 230 degrees. This indicates that when wind blew from the northeast, Monitor A trapped more pollen than Monitor B. Conversely, the data also indicate that when the wind came from the southwest, Monitor B captured more pollen grains than Monitor A.

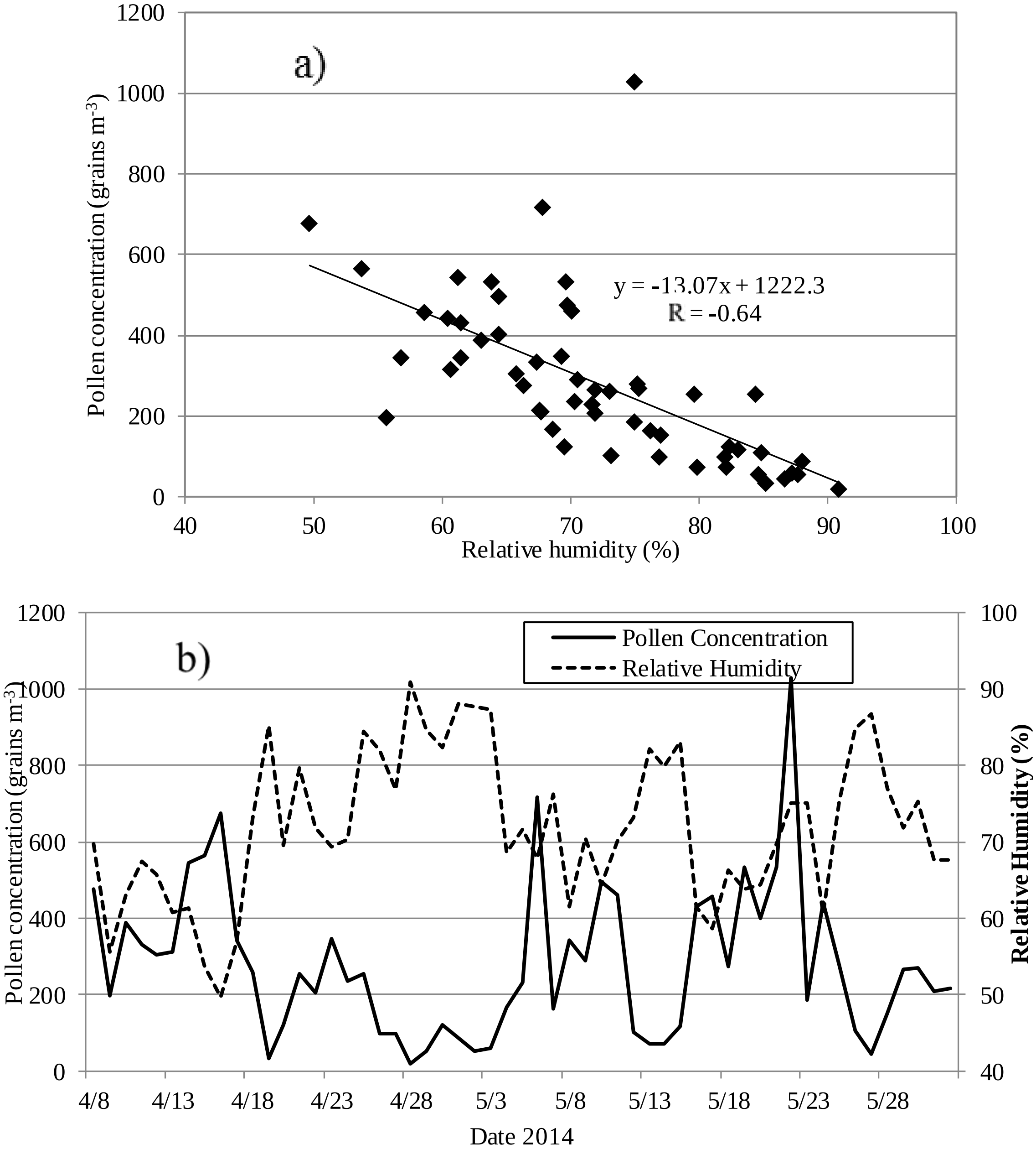

Fig. 2.6 Daily total pollen concentrations observed using Monitor B and daily relative humidity. A) Relationship between total airborne pollen concentrations observed using Monitor B and daily relative humidity; b) daily changes in total airborne pollen concentrations observed using Monitor B and relative humidity.

2.3.4 Findings from the experiment at the Kyoto University Agricultural Science building

In this experiment, an obstacle was placed north of the two anemometers. Therefore, when the horizontal wind direction was north, wind flowing over the obstacle was observed at the vertical anemometer point. Conversely, when the horizontal wind direction was south, the vertical anemometer observed wind flowing toward the obstacle.

Fig. 2.8 shows the relationship between vertical wind speed and horizontal wind direction at hourly (a) and daily (b) resolutions. In these figures, positive numbers for vertical wind speed represent the average vertical velocity of wind flowing downward in a given time. Conversely, negative wind speed in the figure represents the vertical velocity of upward-flowing wind. The experiment shows that, at an hourly scale, wind from the obstacle side flows downward at a probability of 80.7%, and wind from the anemometer side flows upward at a probability of 86.2% (**Fig. 2.8a**). At a daily scale (**Fig. 2.8b**), wind from the obstacle side flows downward at a probability of 72.7%, and wind from the anemometer side flows upward at a probability of 100%. These results suggest that wind flowing from the direction of an obstacle tends to be directed downward and wind flowing toward an obstacle tends to be directed upward, implying that the observed discrepancy in pollen concentrations is caused by altered wind paths.
The north–south Wind Directional Vector ($\boldsymbol{WDV}$) is defined as follows.

$$\boldsymbol{WDV}\,(m\ s^{-1}) = \boldsymbol{WS}\,(m\ s^{-1})\ \times cos(\varphi - WD) \qquad (1)$$

Here, $\boldsymbol{WS}$ represents wind speed (m s^{-1}) and φ is the slant angle from north (in degrees). Because the Kyoto University Agricultural Science building is slanted nine degrees to the east, $\varphi = 9°$ was used in **Fig. 2.9**.

Fig. 2.9 shows $\boldsymbol{WDV}$ plotted against vertical wind speed suggesting that the stronger the wind flows from the obstacle direction, the more the wind path is altered downward, and the stronger the wind toward the obstacle, the stronger the wind path is directed upward. The observed inconsistency of wind flux might be the result of such a recirculation. Thus, **Fig. 2.10** shows the result of the experiment on top of the MeteoSwiss building, indicating that a relationship between the wind directional vectors facing the wall on the MeteoSwiss building and DP exists.

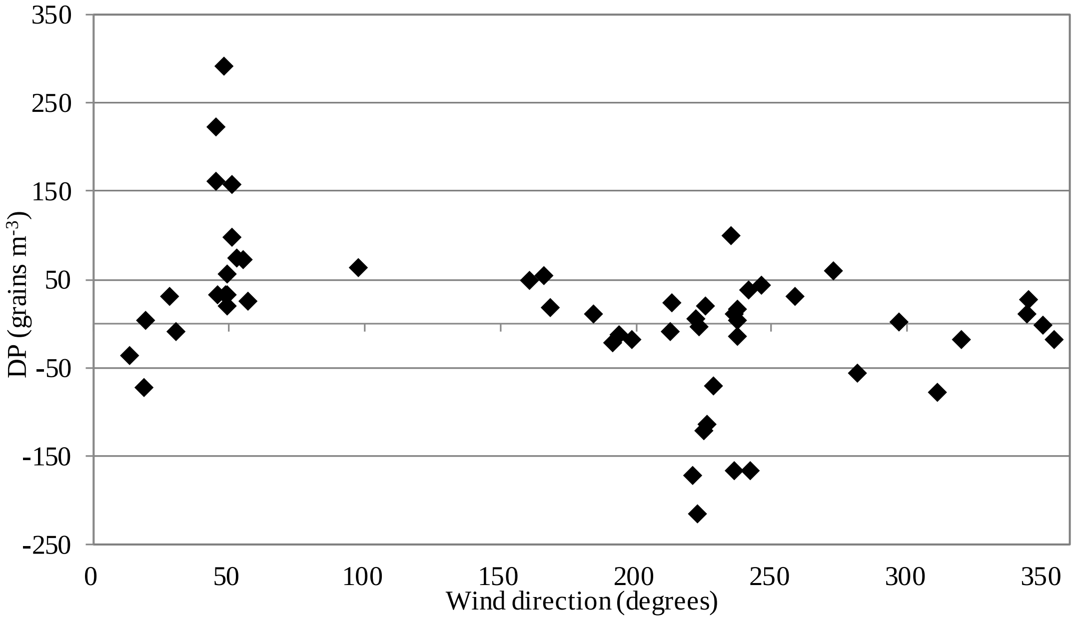

Fig. 2.7 Difference between pollen concentrations (DP) observed by Monitor A and Monitor B and corresponding wind directions.

2.3.5 Findings from the experiment at the MeteoSwiss building

The results above show that wind directions in the examined area have a relatively strong influence on pollen concentrations. **Fig. 2.7** shows the correlation between DP and wind direction, implying that the stronger the wind blew from the northeast, the higher the pollen count recorded by Monitor A. The same is true for Monitor B when the wind was blowing from the southwest. This suggests that the wind directions at which DP shows large values match the direction of the long side of the MeteoSwiss building. Considering the physical characteristics of the building, the pollen sampler equipped with the wind vane intake device is expected to show higher pollen concentrations than the samples equipped with the funnel if the samplers are placed upwind from the wall placed on the rooftop of the building. On the other hand, when the wall is located upwind from the samplers, the pollen monitor equipped with the funnel inlet device is expected to show a higher pollen count than the monitor with the wind vane intake.

A possible reason for the discrepancy in the recorded pollen concentrations is the way in which physical characteristics of the rooftop of the MeteoSwiss building alter the path of the wind. Some researchers have also suggested that the efficiency of bioaerosol monitor inlets varies depending on wind direction and orientation of the intake. For example, Molina *et al*. (2013) showed that environmental factors around pollen monitors have been shown to have some influence on the measurement results using pollen traps. Willeke *et al*. (1992) suggested that when wind flowing toward the pollen samplers exceeds a speed of 93 cm s^{-1}, the pollen samplers' efficiency exceeds 100% showing that the sampler oversampled the pollen concentrations if a vertically oriented inlet is attached to it. On the other hand, when the inlets face upward, the samplers' efficiency decreases to less than 100%. Michel *et al*. (2012) also showed that wind velocity might be the most important factor influencing discrepancies in pollen concentration data. He also mentioned that in order to reduce this discrepancy, pollen monitors oriented in the wind direction should be used. Additionally, some studies have suggested that wind passing over an obstacle creates a recirculation zone downwind from the obstacle [e.g. Gupta *et al*. (2012)].

Considering the findings of Willeke's, Michel's, and Gupta's studies, changes in the efficiency of the pollen samplers are expected to be caused by the way in which an obstacle alters the path of the wind before and after the wind passes over it. The funnel inlet, which is oriented vertically, is expected to show a higher sampling efficiency than the wind vane intake, which is oriented horizontally, as the wind is directed downward toward the monitors as a result of the effect of the obstacle. On the other hand, the funnel inlet is expected to show a lower efficiency in pollen trapping than the wind vane intake since the vertically oriented intake should capture hardly any of the particles blown upward.

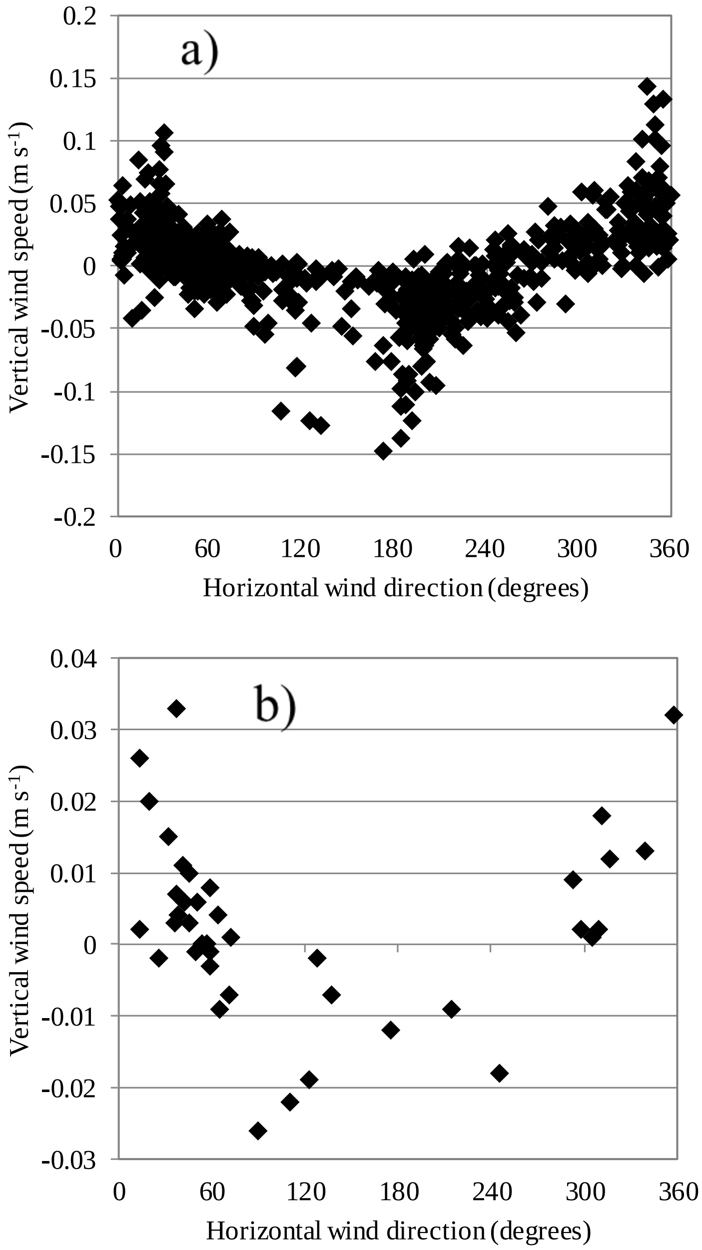

Fig. 2.8 Results of the experiment on top of the Kyoto University Agricultural Science building on a) hourly and b) daily scales.

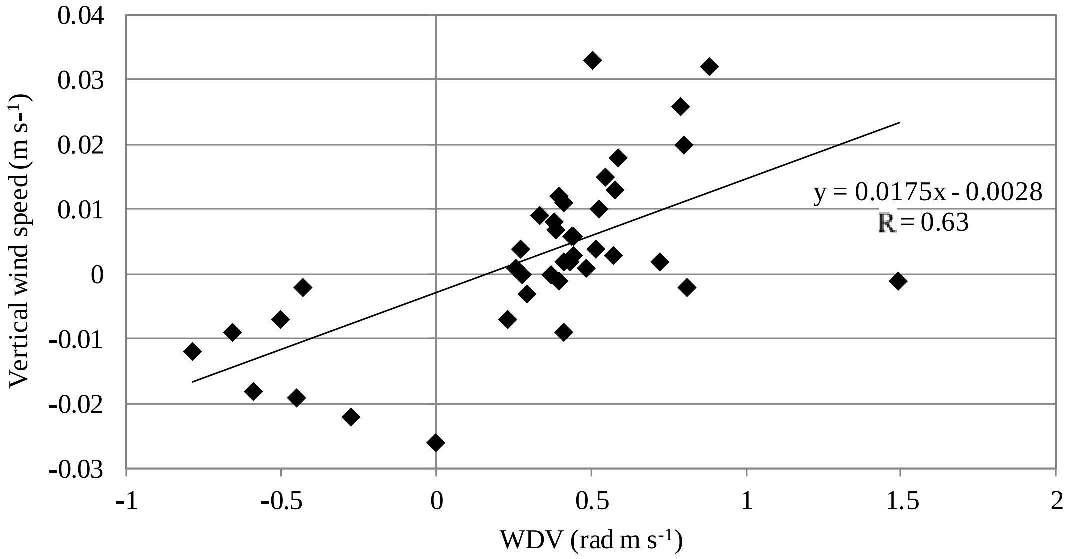

Fig. 2.9 Relationship between horizontal wind directional vectors facing the obstacle and vertical wind speed.

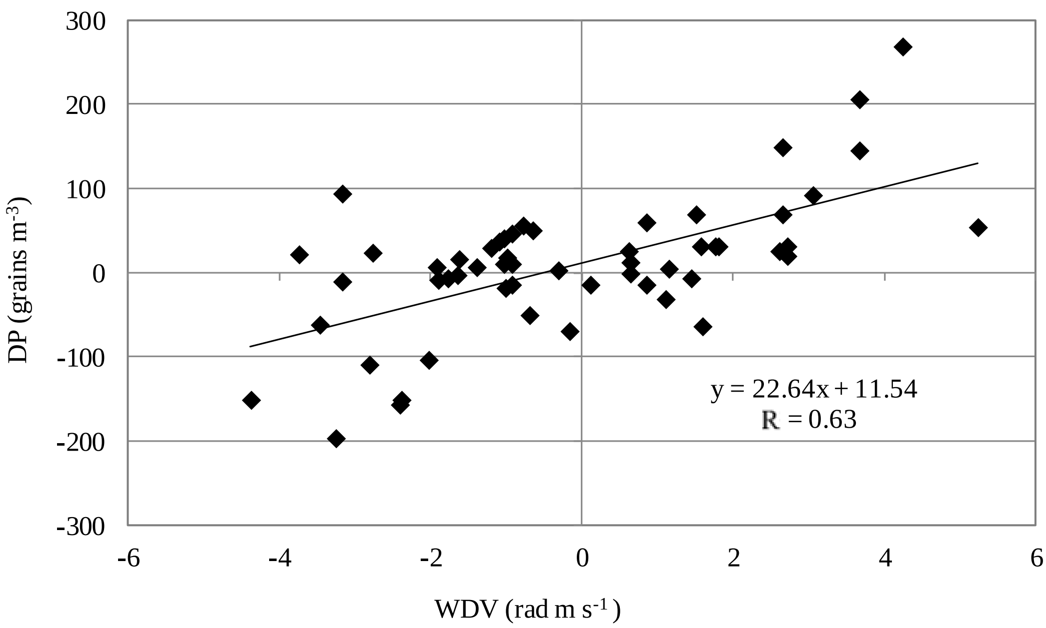

Fig. 2.10 Relationship between pollen concentrations observed by Monitor A and Monitor B and vertical wind vectors facing the wall.

2.3.6 Theoretical model of particle aspiration

Changes in the pollen grain concentration inside an inlet device are likely caused by the difference between particle deposition velocity and air velocity at the inlet plane. Thus, although the aspiration rates of the monitors in this experiment were kept constant at 4.1 L min^{-1}, and the airborne pollen concentration was calculated based on this assumption, the inertial force acting upon the pollen grains might have caused monitors to measure higher or lower airborne pollen concentrations than actually present, because, according to the experiment above, the increase in the horizontal speed of wind flowing over an obstacle leads to an increase in vertical wind speed. Therefore, the inertial force is expected to act upon the pollen in a vertical direction when the wind flows over an obstacle. When a funnel inlet is utilized, the mechanism of condensation and dilution of the pollen concentration (CDP) can be described as shown in Eq. (5) using the equation of continuity (Eq. (2)).

$$CV_A' a = C_0 V_{p0} A \tag{2}$$

where C_0 is the atmospheric pollen concentration (grains m^{-3}), C is the pollen concentration in the suction tube (grains m^{-3}), a is the cross-sectional area of the suction tube (m^2), and A is the cross-sectional area of the orifice of the inlet device (m^2). The symbol V_A' is the aspiration rate at the orifice of the suction tube (m s^{-1}), and V_A and V_{p0} are the aspiration rate (m s^{-1}) and the pollen grain velocity (m s^{-1}) at the orifice of the inlet device, respectively (**Fig. 2.11 (a)**). The equation of continuity of the sampled air holds:

$$V_A' a = V_A A \tag{3}$$

where V_A is the wind velocity at the orifice of the inlet device (m s^{-1}). Thus, by substituting Eq. (3) into Eq. (2), Eq. (4) can be derived:

$$CV_A A = C_0 V_{p0} A \tag{4}$$

Therefore, CDP can be derived as follows:

$$\begin{aligned} CDP &= \frac{C}{C_0} \\ &= \frac{V_{p0} A}{V_A A} \\ &= \frac{V_{p0}}{V_A} \end{aligned} \tag{5}$$

As **Fig. 2.9** suggests that vertical wind velocity at the windward and leeward sides of an obstacle is proportional to horizontal wind velocity, **Fig. 2.10** implies that an increase in horizontal wind speed has a linear influence on the discrepancy in pollen count efficiency, with a correlation coefficient (r) of approximately 0.63. The wind directional vectors were calculated from Eq. (1), although $\varphi = 45$ was used for the equation because the MeteoSwiss building is oriented 45 degrees to the east.

In order to consider the motion of each pollen particle from the Lagrangian point of view, I assumed that τ is the time required for a particle to reach the orifice of the inlet after another particle is sucked into the orifice. Then, the number of particles sucked into the inlet (P) at a given time T (s) is described as follows:

$$P = \frac{T}{\tau} \tag{6}$$

Here, τ is defined as:

$$\tau = \frac{r_m}{V_{p0}} \tag{7}$$

where r_m is the mean free path of pollen grains in the atmosphere (m). When C_A represents the pollen concentration evaluated by the pollen monitor (grains m^{-3}), then C_0 and C_A are described as follows:

$$\begin{aligned} C_0 &= \frac{P}{Q} \\ &= \frac{1}{AV_{p0}T}\frac{V_{p0}T}{r_m} \\ &= \frac{1}{Ar_m} \end{aligned} \tag{8}$$

$$\begin{aligned} C &= \frac{P}{Q_A} \\ &= \frac{1}{AV_AT}\frac{V_{p0}T}{r_m} \\ &= \frac{1}{Ar_m}\frac{V_{p0}}{V_A} \end{aligned} \tag{9}$$

where Q and Q_A are volume of the air pass through the orifice of the inlet and the orifice of the suction tube (m^3), respectively (**Fig. 2.11(b)**). Thus, CDP can be derived as Eq. (10), which leads to the same result as Eq. (5).

$$CDP = \frac{C_A}{C_0} = \frac{A r_m V_{p0}}{A r_m V_A} = \frac{V_{p0}}{V_A} \quad (10)$$

Thus, Eqs. (5) and (10) show that the magnitudes of the discrepancies in the results from different pollen monitors are proportional to V_{p0}, indicating that a CDP above one suggests a measured airborne pollen concentration above the actual airborne pollen concentration. Conversely, when V_{p0} is smaller than V_A, CDP will be smaller than one, showing that the evaluated airborne pollen concentration is smaller than the actual concentration.

In addition to the model discussed above, other models exist. For example, research on particle aspiration by a small inlet was performed by Levin [Levin, 1957; Masuda & Yoshida, 1974]. In Levin's model, the measurement precision is explained to be governed by the inertial force parameter. Vincent (1987) suggested in his model that the aerosol aspiration efficiency is proportional to the air velocity in the direction of the sampler inlet. The accuracy of Vincent's model was subsequently confirmed by an experiment conducted by Li and Lundgren (2002). The model above explains condensation or dilution of airborne particle concentration caused by the inertial force. Especially when wind flows in the direction of the opening of the inlet, the inertial force likely prevents particles from being sucked into the inlet.

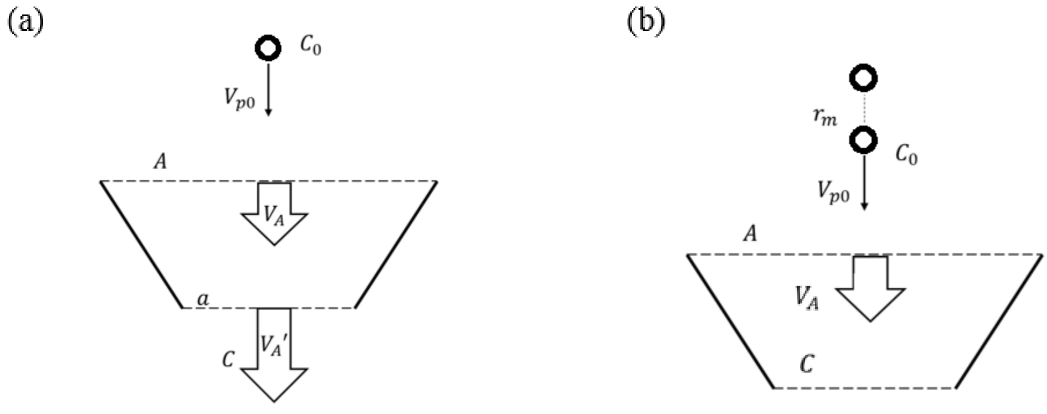

Fig. 2.11 Schematic drawings of wind speed (V_A; $V_A{}'$) (m s^{-1}), pollen concentrations (C; C_0) (grains m^{-3}), and pollen grains velocity (V_{p0}; $V_p{}'$) (m s^{-1}) at the orifice of the inlet with the area of A (m^2) and at the orifice of the suction tube with the area of a (m^2).

2.4 Conclusions

In this study, I analyzed discrepancies in airborne pollen concentration data caused by differences in the physical characteristics of pollen sampler inlets in relationship to meteorological factors. As a result, it appears that micro-scale vertical wind leads to a noticeable discrepancy in airborne pollen concentration data obtained using different types of inlets. This micro-scale vertical wind might be responsible for the discrepancies between airborne pollen concentration data from gravitational samplers such as the Durham sampler and data from volumetric samplers such as the Hirst sampler. Additionally, vertically oriented inlets and horizontally oriented inlets show different airborne pollen concentrations even when they are attached to the same type of volumetric sampler. Thus, my experiments suggest that, when pollen traps are placed on rooftops, the traps should be placed in locations where vertical wind flux is almost zero. Additionally, it is important to understand how far from surrounding obstacles pollen monitors should be placed to improve the acquisition accuracy of airborne pollen concentrations.

Chapter 3

Comparative efficiency of airborne pollen concentration evaluation in two pollen sampler designs related to impaction and changes in internal wind speed

3.1 Introduction

Although reliable sampling of airborne pollen or fungal spores and evaluation of their concentration are required for accurate analysis of their distribution, the best method for determining airborne concentrations is yet to be determined.

Bioaerosol sampling efficiency is significantly influenced by sampling conditions. Thus, to better understand the ideal pollen sampling environment, the relationship between sampling methods and ambient environmental conditions, including local wind speed [Sadyś (2017)], height from ground level [Alcázar and Comtois (2000)], and wind direction [Brixey *et al*. (2005); Li and Lundgren (2002); Sreenath *et al*. (2002); Wen and Ingham (2000)] has been studied. Some studies have considered the relationship between the physical characteristics of sampler inlets and sampling efficiency from an aerosol physics perspective [e.g., Fan *et al.* (1992); Galeev and Zaripov 2003; Grinshpun *et al*. 1994; Hangal and Willeke 1990; Su and Vincent 2002).

Comparison of different pollen samplers is therefore a frequently used and effective research method to better understand sampling efficiency.

In this chapter, I compared two sampling inlets with different designs: an inlet with two layers and a wind-vane-style inlet. Two-layered sampling inlets are designed to cancel the effect of wind speed by blocking particle trajectories inside the inlets and have been used in aerosol sampling experiments [e.g. Ballach *et al*. (1999); Kreissl *et al*. (1991)]. Wind vane inlets, such as the Hirst-style sampler used here, are designed to sample particles from an upwind direction. By comparing these two types of inlets, I examined the discrepancies between the actual and evaluated pollen concentrations caused by the sampling device to elucidate the possible mechanism that causes the inaccuracy in the pollen concentration.

3.2 Materials and methods

3.2.1. Data acquisition

To compare the sampling efficiencies of each sampling inlet, I used airborne pollen concentrations determined by a KH-3000-01 pollen monitor (Yamatronics, Japan) located on the top of the MeteoSwiss building in Payerne, Switzerland (46°48’48’’N, 6°56’35’’E). The KH-3000-01 uses laser scattering to evaluate total airborne pollen concentration, calculated by converting pollen counts collected at a sampling rate of 4.1 L min^{-1} to grains m^{-3}. Sampling was carried out from July 15 to August 20, 2016 and from March 10 to July 31, 2017. The 2016 sampling period was limited because of certain technical problems. Further details are provided in Kawashima et al. (2007; 2017).

For the two-layered inlet, I used a Sigma-2 passive sampler (Particle Vision, Switzerland). This device has two parts, i.e. a protective hood with a diameter of 155 mm overlapping a cylinder with a diameter of 100 mm (**Fig. 3.1(a)**). Both parts have four 37 mm × 70 mm inlet openings, offset between the layers to eliminate the effects of wind on the interior cylinder. The wind vane inlet, a Hirst-style sampler inlet (MeteoSwiss), set up next to the two-layered sampling inlet, uses a vane to orient the inlet in an upwind direction, funneling air into a sampling tube with a diameter of 5 mm (**Fig. 3.1(b)**). Each device was linked to a separate KH-3000-01 unit.

I performed independent pollen sampling at the experimental site using the Hirst sampler for data confirmation. Although the KH-3000-01 monitors automatically total airborne pollen concentration, the Hirst unit can preserve samples of airborne pollen grains on sampling slides, allowing manual counting and identification. I could thus identify the pollen taxa present during the study period and could calculate the daily or total average pollen grain size. Additionally, some meteorological factors, such as humidity, temperature, precipitation, day length, and wind speed and direction, were recorded at the experimental site by MeteoSwiss. I used wind speed and direction data based on the service of MeteoSwiss.

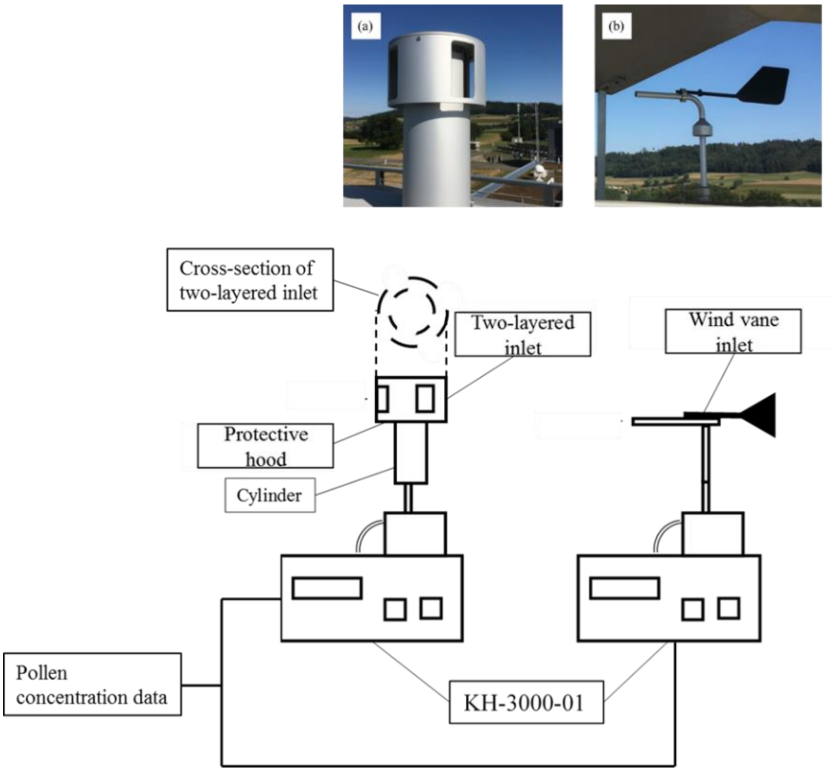

Fig. 3.1 Photograph of (a) Sigma-2 two-layered sampling inlet and (b) Hirst-style wind vane inlet, and schematic drawing of the experimental set up: two-layered sampling inlet (left) and wind vane inlet (right) attached to KH-3000-01.

3.2.2 Conversion theory

The relationship between the sampling efficiency of the Sigma-2 two-layered and Hirst-style wind vane sampling inlets can be expressed by the continuity equation of pollen flux with the assumption that the wind vane sampling inlet evaluate the actual airborne pollen concentration:

$$C_S v_S a = C_0 v_0 A - Bl - Ex \tag{11}$$

where C_0 is the airborne pollen concentration in the atmosphere, C_S is the pollen concentration inside the two-layered sampling inlet cylinder, v_S is the wind speed toward the KH-3000-01 suction tube, a is the cross-sectional area of the two-layered sampling inlet cylinder, v_0 is the wind speed inside the two-layered sampling inlet protective hood, A is the effective area of the two-layered sampling inlet ports, Bl is the number of pollen grains blocked by the wall inside the two-layered sampling inlet protective hood, and Ex is the number of pollen grains passing through the two-layered sampling inlet without being sampled.

From Eq. (11), the relationship between the two-layered sampling inlet evaluation results and the pollen concentration in the atmosphere is expressed as:

$$C_S = \frac{C_0 v_0 A - Bl - Ex}{v_S a} \tag{12}$$

The amount of air entering the cylinder is almost equal to that flowing out from the bottom of the cylinder, because the sampling rate is less than the air flow rate in the cylinder. Thus, it is reasonable to assume that wind speed in the two-layered sampling inlet cylinder is proportional to wind speed entering the two-layered sampling inlet protective hood, expressed as $v_S = Xv_0$, where X is a coefficient. With these assumptions, Eq. (12) becomes:

$$C_S = \frac{C_0 v_0 A - Bl - Ex}{X v_0 a} \tag{13}$$

Therefore, X is written as:

$$X = \frac{C_0 v_0 A - Bl - Ex}{C_S v_0 a} \tag{14}$$

It is possible to calculate a directly, since the two-layered sampling inlet cylinder has a radius of 50 mm. When the wind flows from direction θ (**Fig. 3.2**), the effective value of A is calculated as:

$$A = Wh\left\{cos\theta + \cos\left(\frac{\pi}{2} - \theta\right)\right\} \quad (-\frac{\pi}{2} \leq \theta < 0) \tag{15}$$

where W is the port's width ($= 37$ mm), and h is its height ($= 70$ mm).

By defining φ as:

$$\varphi = \theta + \pi/4 \tag{16}$$

Eq. (16) gives:

$$A = Wh\left\{cos\left(\frac{\pi}{4} - \varphi\right) + cos\left(\frac{\pi}{4} + \varphi\right)\right\} \quad (-\frac{\pi}{4} \leq \varphi < \frac{\pi}{4})$$
$$= 2Whcos\frac{\pi}{4}\cos\varphi \tag{17}$$
$$= \sqrt{2}Whcos\varphi$$

Thus, the expected value of A can be calculated under the assumption that the wind flows equally from all directions:

$$E[A] = \sqrt{2}Wh \times 2\int_{-\frac{1}{4}}^{\frac{1}{4}} cosx\pi dx$$
$$= \frac{2\sqrt{2}Wh}{\pi}[sinx\pi]_{-\frac{1}{4}}^{\frac{1}{4}} \tag{18}$$
$$= \frac{4Wh}{\pi}$$

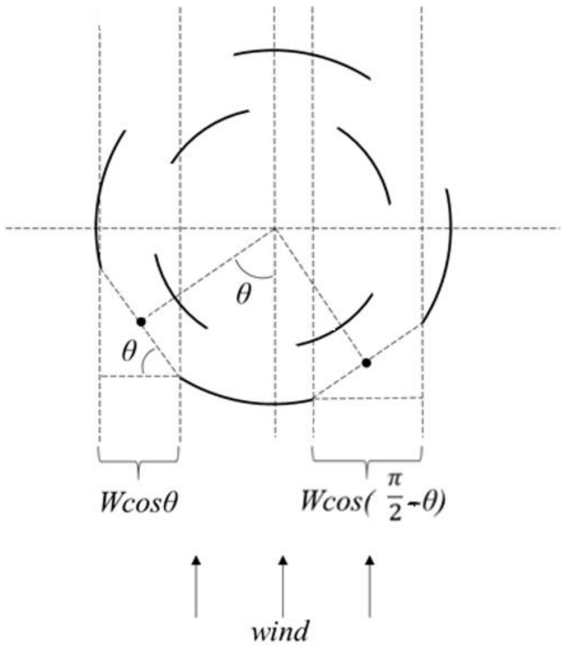

Fig. 3.2 Effective sampling area for the two-layered sampling inlet with wind from direction θ.

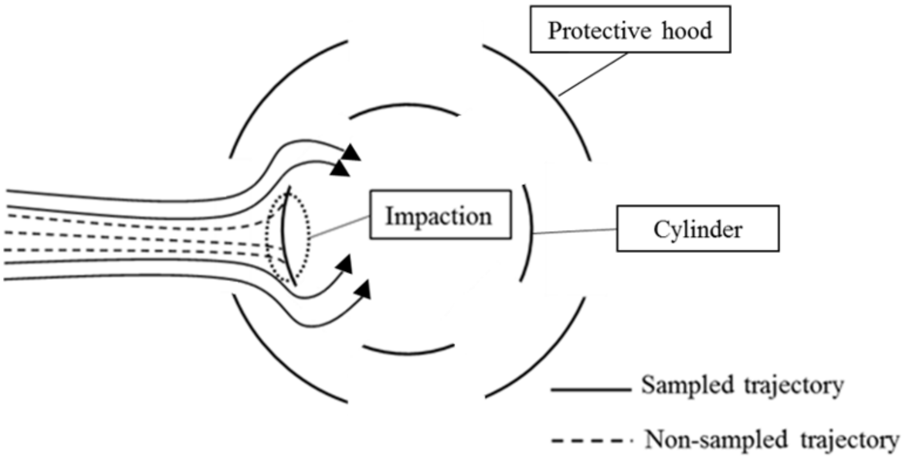

Fig. 3.3 Schematic diagram of pollen impaction in the two-layered inlet. Some airborne pollen grains encountering the sampler from the left pass through ports in the protective hood and cylinder, where they are sampled (solid flow lines), while others pass the hood but are blocked by the cylinder wall (dotted flow lines).

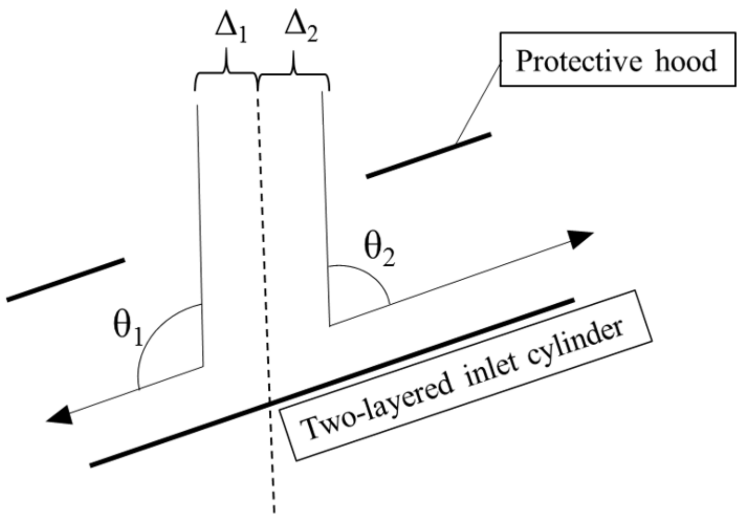

Fig. 3.4 Schematic diagram of wind entering the two-layered sampling inlet port from direction θ_1 (θ_2).

Although it is not possible to directly calculate Bl, an approximation can be made by assuming that the ejection of pollen grains from the two-layered inlet is mostly caused by impaction inside the protective hood (**Fig. 3.3**). This impaction theory was introduced by Hinds (1999) and is described as:

$$\begin{aligned} P &= 1 - I \\ I &= \frac{\pi\tau v_0}{W} \\ \tau &= \left(\frac{d^2\gamma C_C}{18\eta}\right)\left(\frac{24}{C_D Re_p}\right) \\ C_D &= \frac{F_D}{\frac{1}{2}\rho {v_0}^2 A_p} \end{aligned} \tag{19}$$

where P is the probability of a particle not being impacted, I is the probability of impaction, τ is the relaxation time (s), γ is the density of pollen grains ($= 1.0 \times 10^3$ kg m^{-3}), d is the pollen grain diameter (m), C_C is the Cunningham correction factor, η is the viscosity of the air ($= 1.8 \times 10^{-5}$ kg m^{-1} s^{-2}), C_D is the drag coefficient, F_D is the drag force (N), ρ is the air density (kg m^{-3}), and A_p is the cross-sectional area of a pollen grain. By applying this assumption (that the ejection of pollen grains is caused by impaction), Eq. (13) becomes:

$$\begin{aligned} C_S &= \frac{C_0 v_0 E[A] - Bl}{v_S a} - \frac{Ex}{X v_0 a} \\ &= \frac{C_0 v_0 E[A](1 - I)}{X v_0 a} - \frac{Ex}{X v_0 a} \\ &= \frac{C_0 (1 - I)}{X}\frac{E[A]}{a} - \frac{Ex}{X v_0 a} \end{aligned} \tag{20}$$

For the manipulation of I in Eq. (19), the port orthographic width to the wind direction (W_o) should be substituted as W. Similar to Eq. (18), the expected value of W is calculated under the assumption that the wind flows equally from every direction:

$$\begin{aligned} E[W_o] &= \frac{2W}{\pi}\int_0^{\frac{\pi}{2}} sinx dx \\ &= \frac{2W}{\pi} \end{aligned} \tag{21}$$

When the wind flows at generalized angles (θ_1, θ_2) (**Fig. 3.4**), P is calculated as:

$$P = 1 - \left(\frac{\Delta_1 + \Delta_2}{W_o}\right) \tag{22}$$

$$\Delta_1 = \tau\left(\frac{{v_0}^2}{r}\right)\left(2\pi r \cdot \frac{\theta_1}{2\pi}\right)\frac{1}{v_0} \tag{23}$$

$$\Delta_2 = \tau\left(\frac{{v_0}^2}{r}\right)\left(2\pi r \cdot \frac{\theta_2}{2\pi}\right)\frac{1}{v_0} \tag{24}$$

$$\theta_1 + \theta_2 = \pi \tag{25}$$

where r is the radius of the circular arc of the air impacting on the two-layered inlet cylinder.

Additionally, although θ_1 and θ_2 are variables, the sum of the two variables is constantly π. Thus, Eqs. (23–25) give:

$$\begin{aligned}\Delta_1 + \Delta_2 &= \tau\left(\frac{{v_0}^2}{r}\right)\left(2\pi r \cdot \frac{\theta_1 + \theta_2}{2\pi}\right)\frac{1}{v_0} \\ &= \pi\tau v_0\end{aligned} \tag{26}$$

This suggests that the width of the limiting trajectory for the impaction is constant, $\pi\tau v_0$.

Thus, a general form of P is given as:

$$P = 1 - \frac{\pi\tau v_0}{W_o} \tag{27}$$

Because Eq. (27) contains a generality when n number of ports are exposed to the wind, it can be converted without loss of generality to give the total probability of the avoidance of the impaction, P_{total}, calculated as:

$$\begin{aligned}P_{total} &= 1 - \frac{\sum_{k=1}^{n}\left(\Delta_1^k + \Delta_2^k\right)}{nE[W_o]} \\ &= 1 - \frac{n\pi^2\tau v_0}{2nW} \\ &= 1 - \frac{\pi^2\tau v_0}{2W}\end{aligned} \tag{28}$$

which shows that the probability of impaction avoidance is independent of the number of ports and wind direction.

Furthermore, it is reasonable to assume that the number of pollen grains ejected from the two-layered sampling inlet hood without being sampled is proportional to the number of pollen grains passing into the cylinder. Thus:

$$Ex = \varepsilon C_0 v_0 E[A] \tag{29}$$

where ε is the coefficient. This gives the following equation:

$$\begin{aligned} X &= \frac{P_{total} C_0}{C_S} \frac{E[A]}{a} - \frac{\varepsilon C_0 v_0}{C_S v_0} \frac{E[A]}{a} \\ &= (P_{total} - \varepsilon) \frac{C_0}{C_S} \frac{E[A]}{a} \end{aligned} \tag{30}$$

Although it is not possible to theoretically calculate ε in most cases, the approximate X value would be given directly by substituting the value at which the total pollen count of the two-layered sampling inlet is equal to that of the theoretical two-layered inlet. Regarding our experimental results, I assumed that the evaluation results from the wind vane inlet represent C_0 and those from the Sigma-2 two-layered sampling inlet represent C_S. In other words, the conversion results of the wind vane inlet are treated as theoretical two-layered inlets in this study.

As the wind should decelerate upon entering the two-layered sampling inlet port, I introduced the deceleration ratio (m) to manipulate wind speed inside the two-layered sampling inlet protective hood, allowing the relationship between v_0 and U to be $v_0 = mU$. Therefore, the probability of impaction avoidance is calculated as:

$$\begin{aligned} P_{total} &= 1 - \frac{\pi^2 \tau v_0}{2W} \\ &= 1 - \frac{m\pi^2 \tau U}{2W} \end{aligned} \tag{31}$$

In this study, m was optimized by nonlinear optimization for the correlation coefficient to have the highest value.

The theoretical two-layered inlet was calculated in the same way for both the 2016 and 2017 data. However, for the 2016 data, the average pollen grain size throughout the sampling period (23.5 μm) was substituted for d because this period lasted only one month and no seasonal change in vegetation was observed. For the 2017 data, the daily average pollen grain size was substituted for d, because some seasonal changes in the vegetation were observed during the 2017 sampling period.

3.2.3 Introduction of mechanical mobility

The wind speed inside the Sigma-2 cylinder is expected to be lower than that outside. Thus, laminar flow should be dominant inside the cylinder in which the adherence of pollen grains to a given flow line governs their movement. To better account for the changes in the pollen size in 2017, I introduced the concept of mechanical mobility (μ), which is an indicator for the adherence of a particle to a flow line:

$$\mu = \frac{1}{3\pi d\eta} \tag{32}$$

This was applied to the experimental data by substituting the daily average pollen grain size for d. Furthermore, the mechanical mobility was multiplied by the average pollen diameter ($d_{average}$) for unit adjustment (M):

$$\begin{aligned} M &= \frac{3\pi d_{average}\eta}{3\pi d\eta} \\ &= \frac{d_{average}}{d} \end{aligned} \tag{33}$$

Thus, to calculate the theoretical two-layered inlet for 2017, both mechanical mobility and impaction theory were applied to the airborne pollen concentration datasets from the wind vane inlet.

3.3 Results and discussion

3.3.1 2016 results

During the 2016 sampling period, the highest daily pollen concentration was observed on July 20 by both the two-layered (798.7 grains m^{-3}) and the wind vane (245.8 grains m^{-3}) sampling inlets (**Fig. 3.5a**). After this peak, the daily concentrations followed a roughly weekly cycle. The relationship between the pollen concentrations evaluated by the two-layered and wind vane inlets showed that the sampling efficiency of the two-layered sampling inlet was approximately three times higher than that of the wind vane inlet at a daily scale (**Fig. 3.5b**). Urticaceae was the dominant taxon during the sampling period, representing 68.0% of all sampled airborne pollen grains, followed by Poaceae, *Plantago*, and *Zea* (**Fig. 3.6a**).

When impaction theory was applied and 0.112 and 0.73 were substituted for X and m, respectively, the correlation coefficient between two-layered and theoretical two-layered inlets was the highest (**Fig. 3.7**). This implied that the wind speed inside the two-layered inlet cylinder was reduced to approximately 8% of the wind speed entering the two-layered sampling inlet port, calculated as mX.

3.3.2 2017 results

During the 2017 sampling period, the highest daily pollen concentration was observed on July 19 by both the two-layered (278 grains m^{-3}) and wind vane (113 grains m^{-3}) sampling inlets (**Fig. 3.8a**). As in 2016, both inlets recorded similar pollen concentration trends during the sampling period. However, technical problems produced some data gaps: Pollen concentration data from the two-layered sampling inlet are missing from April 10 to 24, those from the wind vane inlet are missing from May 9 to 14, and those from both samplers are missing from July 3 to 11. The sampling efficiency of the two-layered sampling inlet was approximately 1.36 times higher than that of the wind vane inlet (**Fig. 3.8b**). Poaceae and *Quercus* were the most dominant taxa, representing 21.3% and 19.6% of the sampled pollen grains, respectively (**Fig. 3.6b**).

The sampling efficiency ratio of the two-layered to wind vane inlets became relatively larger in the latter half of the sampling period (**Fig. 3.9**). **Fig 3.9** also shows the reciprocal number of the daily average of the pollen diameter. This value tracked changes in the relative sampling efficiency of the two-layered sampling inlet, suggesting that increases in pollen diameter would result in decreased sampling efficiency for this inlet. The tracking is illustrated in the relationship between the weekly changes in geometric averages of these two values (**Fig. 3.10**). The changes in the daily average of the pollen diameter is observed because of the vegetation changes. Here, the pollen grain diameters of each taxon were obtained from the Paldat palynological database (2000 onwards, www.paldat.org).

Furthermore, the re-optimization of m and X resulted in a more generalized optimization in which 0.63 was substituted for m. Applying impaction theory to the 2017 wind vane inlet data was effective for the conversion of these results to two-layered inlet results (**Fig. 3.11a**). The slope of the approximation straight line became 0.907 when $X = 0.167$. Moreover, the mechanical mobility allowed the theoretical two-layered inlet to reflect the observed two-layered inlet more accurately (**Fig. 3.11b**), although the slope of the approximated straight line became smaller, because multiplying the theoretical two-layered inlet values by M enlarges the average value of the theoretical two-layered inlet.

Our results show that although the 2016 experimental results originally indicated a clear relationship between the sampling efficiency of the two samplers, the application of impaction theory further improved the correlation coefficient, suggesting that impaction occurs inside the two-layered sampling inlet protective hood. This is also true for the 2017 results, which suggests that it was possible to consider the changes in pollen sizes by applying mechanical mobility.

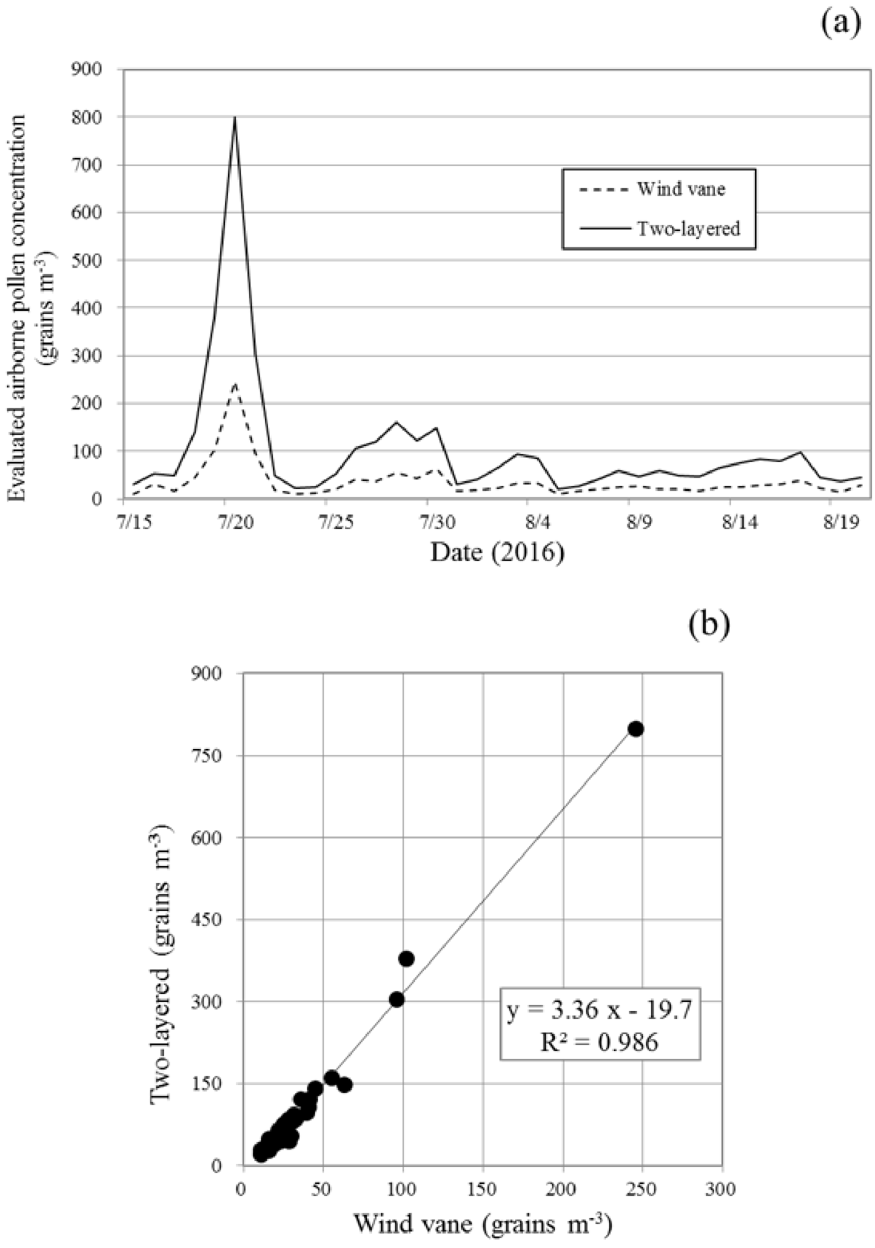

$p < 0.05$

Fig. 3.5 (a) Daily changes in airborne pollen concentration collected by wind vane and two-layered sampling inlets in 2016 and (b) their relationship.

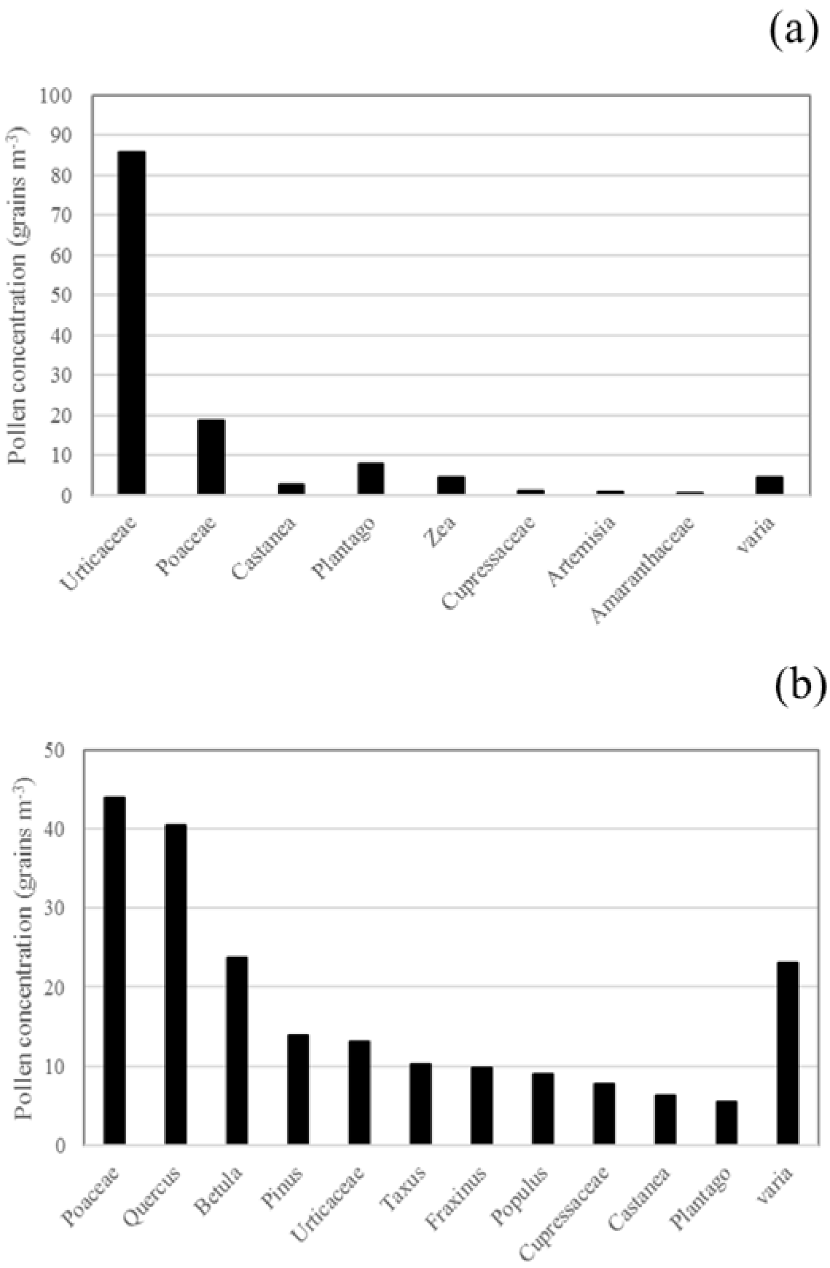

Fig. 3.6 Taxa and grain counts for pollen collected from (a) July 15 to August 20, 2016 and (b) March 10 to July 31, 2017 by a Hirst sampler; identification and counts were performed by visual observation.

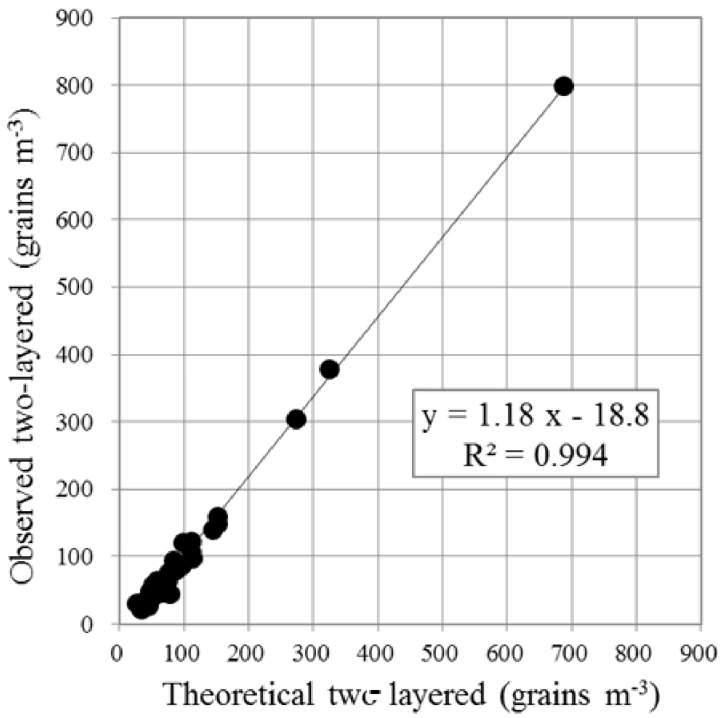

$p < 0.05$

Fig. 3.7 Relationship between airborne pollen concentrations observed using the two-layered sampling inlet in 2016 and results from applying impaction theory to airborne pollen concentrations observed by the wind vane inlet.

(a)

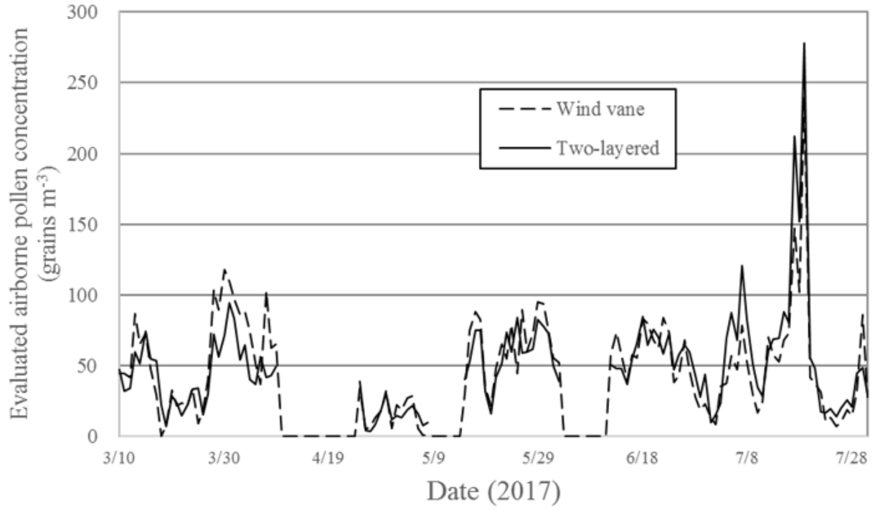

(b)

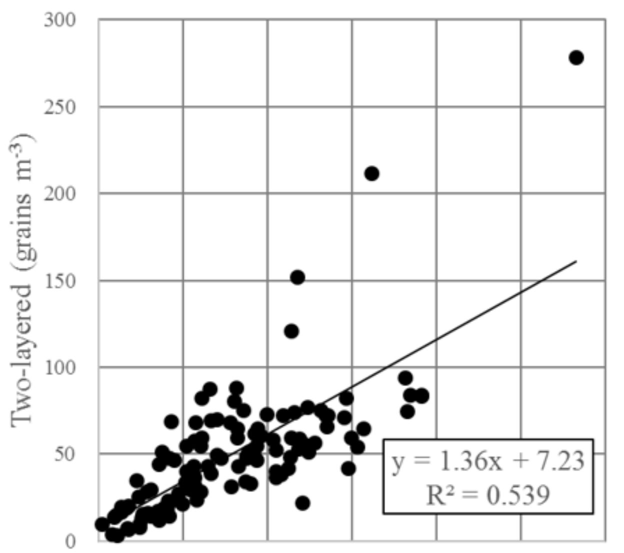

$p < 0.05$

Fig. 3.8 (a) Relationship between sampling efficiency of wind vane and two-layered sampling inlets in 2017 and (b) their relationship.

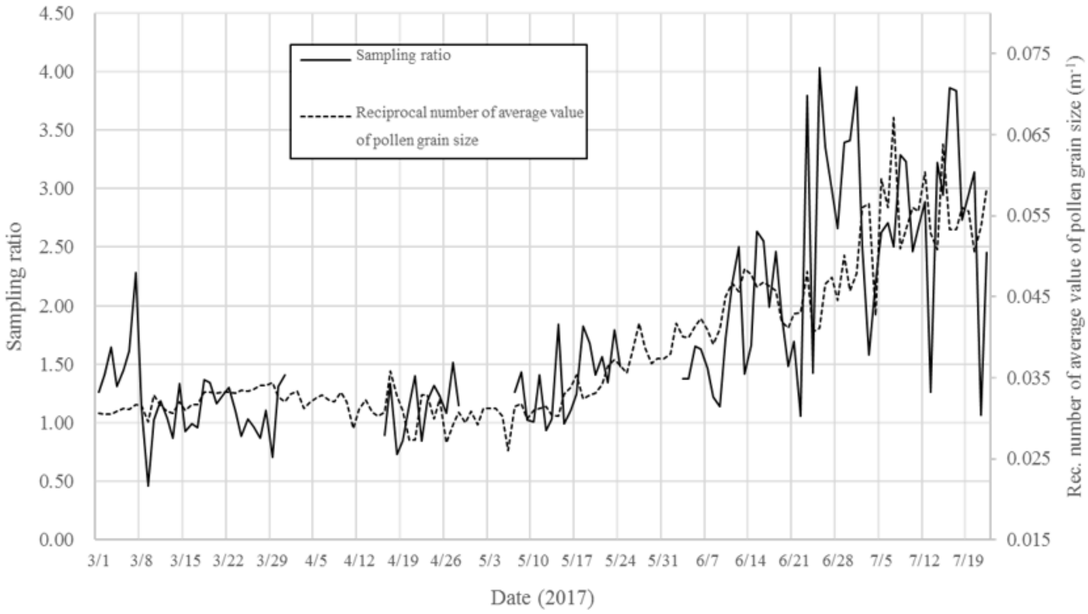

Fig. 3.9 Daily changes in sampling ratio between the two-layered and wind vane sampling inlets along with the reciprocal number of the average value of pollen size during the 2017 sampling period.

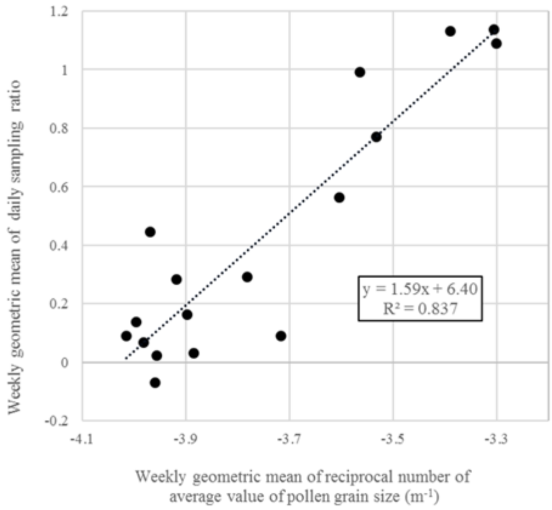

$p < 0.05$

Fig. 3.10 Relationship between weekly geometric mean of daily sampling ratio between the two-layered and wind vane inlets and weekly geometric means of reciprocal number of the average pollen size.

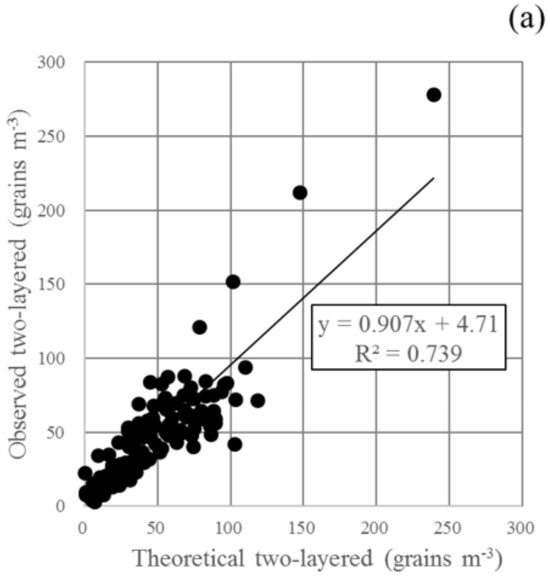

$p < 0.05$

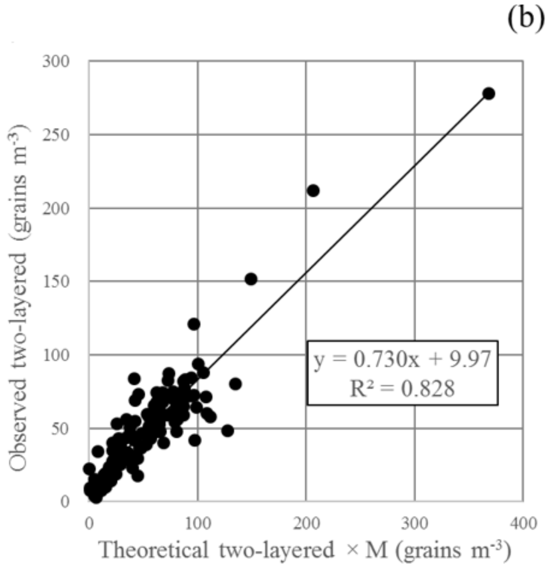

$p < 0.05$

Fig. 3.11 (a) relationship between airborne pollen concentrations observed using the two-layered in 2017 and results from applying impaction theory to airborne pollen concentrations observed by the wind vane inlet (theoretical two-layered inlet). (b) Results from applying mechanical mobility and impaction theory to wind vane airborne pollen evaluation.

3.4 Conclusions

I showed that pollen sampling using the Sigma-2 two-layered sampling inlet was more efficient than that using a Hirst-style wind vane inlet during spring and summer in Payerne, Switzerland. The higher sampling efficiency of the two-layered sampling inlet seemed to be caused by changes in wind speed inside the sampling inlet. Additionally, the two-layered sampling inlet protective hood apparently produced impaction effects causing discrepancies in sampling efficiency. Finally, changes in pollen diameter influenced the sampling efficiency due to changes in grain adherence to flow lines.

Thus, our experimental results show that the pollen concentration evaluated by a pollen sampler has some inaccuracies caused by the sampling device itself, and I theoretically explained the possible mechanism that causes the altered evaluation results from the two-layered pollen sampling inlet. The application of our findings will help to improve the accuracy of pollen sampling regardless of phenological changes in pollen grain size and changes in wind speed.

Chapter 4

Evaluating inaccurate pollen concentrations caused by turbulent vertical flux

4.1 Introduction

In previous chapters, the sampling efficiencies of volumetric samplers were discussed. However, as mentioned in Chapter 1, comparison of volumetric samplers and gravitational sampler is very important for the quality control of allergen monitoring. In order to understand the health impact of allergic pollen to humans, volumetric samplers, which are designed to imitate the respiratory function, have been widely used for pollen sampling [e.g. Camacho *et al*. (2017); Carinanos *et al*. (2002); Hrga *et al*. (2010); Monroy-Colin *et al*. (2018); Moreno-Grau *et al*. (1998)]. The gravitational method is also another frequently used method; it is employed not only to understand the deposition quantity of pollen but because of its simplicity [e.g. Hofmann *et al*. (2016); Tosunoğlu *et al.* (2013)]. Gravitational samplers are also used to understand pollen deposition on patients' skin [Erkara *et al*. 2009].

Previous studies have shown that the pollen concentrations evaluated by volumetric samplers and passive samplers have clear correlations [Bricchi *et al*. (2000); Sun *et al*. (2017)]. Conversely, it has been stated that the volumetric method and the gravitational method have virtually no correlation [Cornell *et al*. (1961)]. Thus, there are discrepancies in the evaluations of pollen sampling efficiencies of the gravitational sampling methods among previous research.

In this study, the two most frequently used pollen sampling methods—a volumetric method called the Hirst sampler, which is the most commonly used volumetric sampler, and a gravitational method called the Durham sampler, which is the most commonly used gravitational sampler—were compared to re-evaluate the existing comparison method between the gravitational method and the volumetric method.

4.2. Materials and methods

4.2.1 Experimental setup

The Hirst sampler and the Durham sampler (**Fig. 4.1**) were permanently set on the rooftop of the Hokkaido Institute of Public Health (43° 4' 59'' N, 141° 19' 59'' E). The sampling rate of the Hirst sampler was set at 10 L min^{-1}. Pollen grains sampled by these devices were counted and sorted through visual observation using a microscope (Olympus BX 53-F, Tokyo, Japan). Although all pollen taxa in the atmosphere were sampled, *Betula* was chosen as the study object because of its representativeness as the main allergenic pollen. The *Betula* pollen sampling was performed throughout the period April 20th to May 20th annually, from 2013 to 2016. Because forests were situated to the north of the sampling site, in order to obtain clear data without background errors, I used data collected only when the daily dominant wind direction was not from the north. Additionally, some daily data were missing because of technical problems with the Hirst sampler.

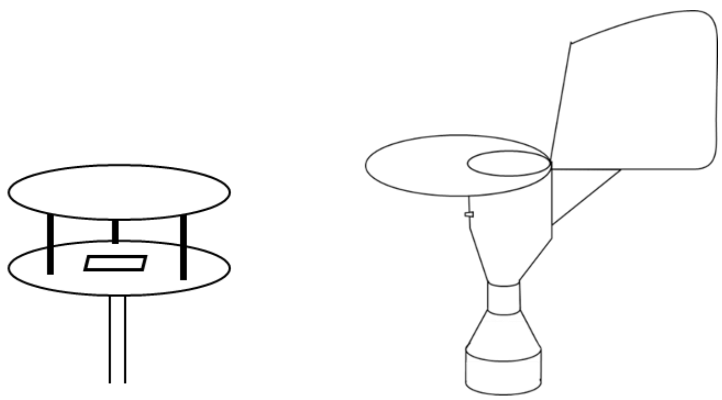

Fig. 4.1 The Durham sampler (left) the Hirst sampler (right).

4.2.2 Theory

A method to determine the airborne pollen concentration from sampling results was first introduced by Scheppegrell (1917), and subsequently improved by Cocke (1937) and Feinberg and Steinberg (1933) as follows:

$$C_G = \frac{n_G}{v_f \times a \times t} \quad (34)$$

where n_G is the number of deposited pollen grains, v_f is the pollen falling speed (m s^{-1}), a is the sampling area (m^2), t is the sampling duration (s), and C_G is the atmospheric pollen concentration (grains m^{-3}). For v_f, the terminal velocity derived from Stokes' law is usually substituted, which is calculated as,

$$v_f = \frac{2r_p^2(\rho_p - \rho_f)g}{9\eta} \tag{35}$$

where r_p is the radius of a particle (m), ρ_p is the density of the particle (kg m^{-3}), ρ_f is the density of fluid (kg m^{-3}), and η is the viscosity of the ambient fluid (m^2 s^{-1}). Because the radius of a pollen grain varies, a representative pollen grain radius that fit the experiment best was calculated and substituted; specifically, $r_p = 17$ (μm).

I used these equations for the conversion of gravitational sampling results from the Durham sampler to the airborne pollen concentration. For the density of pollen grains, 1 (g cm^{-3}) was substituted.

4.3 Results

The airborne pollen concentration data from the gravitational sampler and the volumetric sampler exhibited high correlations especially in 2013 and 2016, showing that in these two years, the identification and counting of *Betula* pollen for both the gravitational sampler and the volumetric sampler were performed precisely, whereas the correlation coefficients for 2014 and 2015 are relatively low (r^2=0.967 (2013); r^2=0.556 (2014); r^2=0.467 (2015); r^2=0.973 (2016)) (**Fig. 4.2**). Only a limited amount of data is available for 2013 because the volumetric sampling was performed only from May 9th because of a technical problem. The slopes of the scatter plots of the volumetric sampling data and the converted gravitational sampling data show differences in sampling efficiencies, which are ratios of the sampling efficiency of the gravitational sampling efficiency to that of the volumetric sampling efficiency. These results indicate that the converted gravitational sampling results tend to exhibit higher airborne pollen concentrations than the volumetric sampling method.

The correlations between the sampling ratio of the gravitational method to the volumetric method and the ratio of wind speed, which is a significant meteorological factor for particle samplings, to the sampling rate, which was constant, are also shown in scatter plots (**Fig. 4.3**). In these plots, proportional relations are shown (r^2=0.452 (2013); r^2=0.400 (2014); r^2=0.016 (2015); r^2=0.563 (2016)).

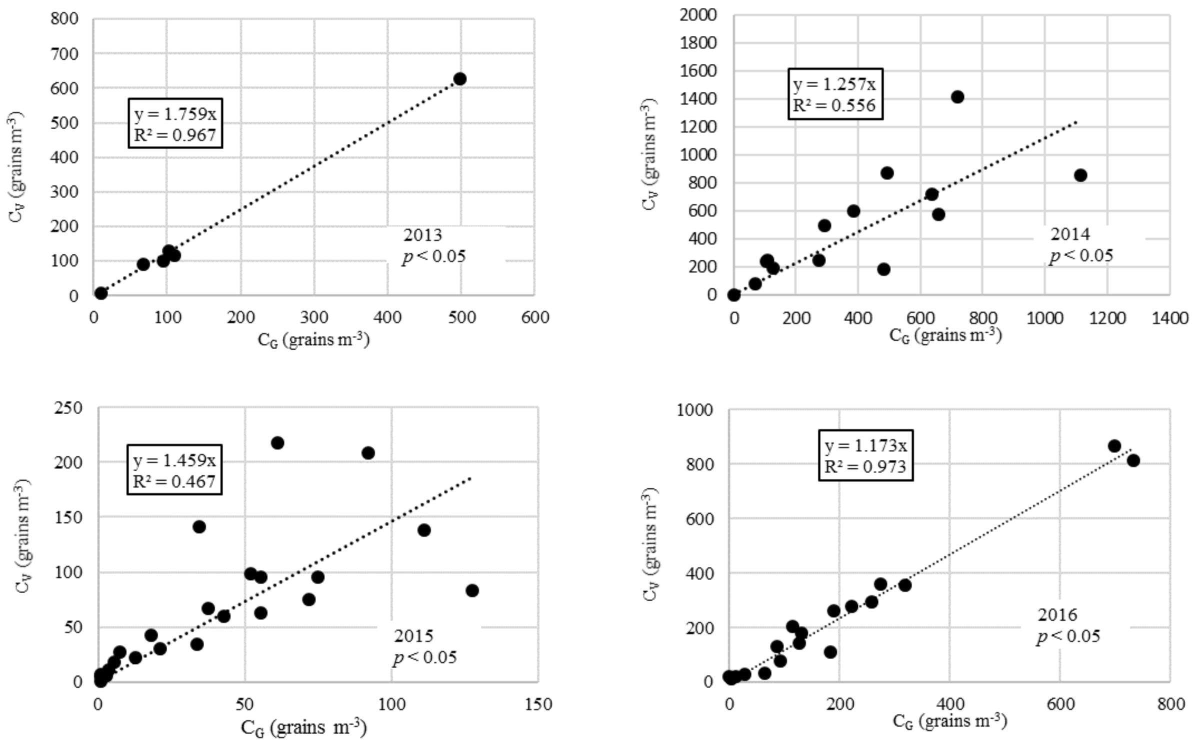

Fig. 4.2 Relationship between airborne pollen concentration evaluated from volumetric sampling results and gravitational sampling results.

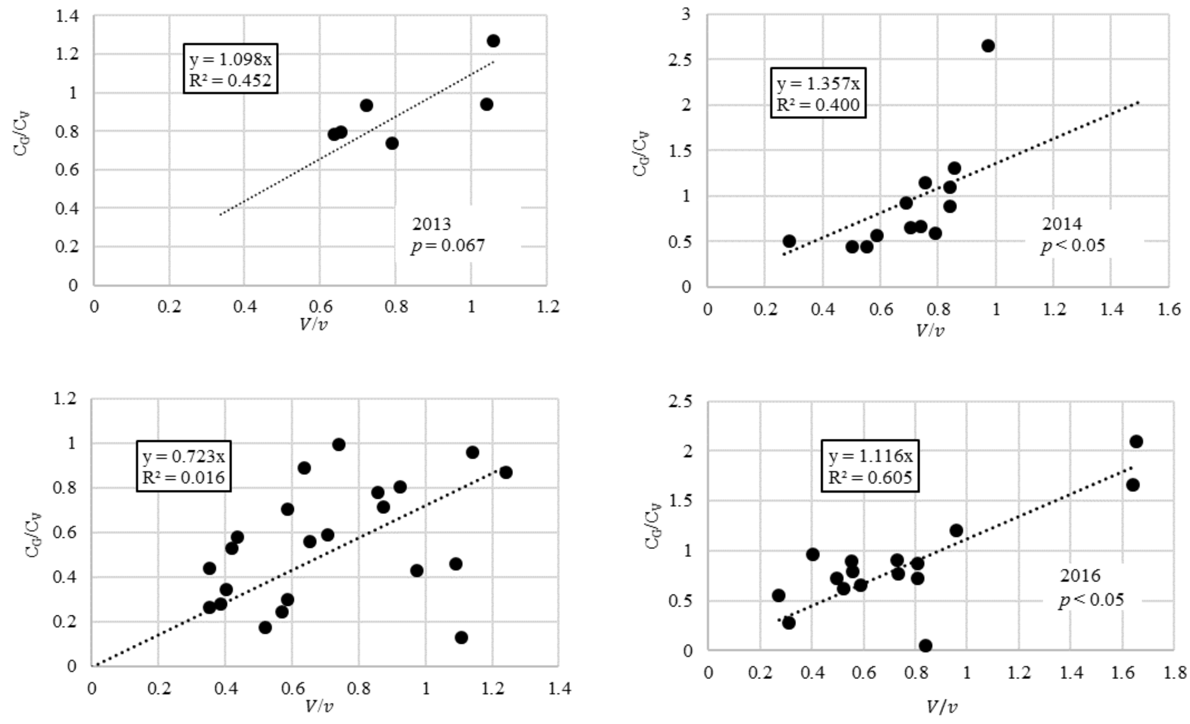

Fig. 4.3 Relationship between ratio of evaluated airborne pollen concentration of gravitational sampling to that of volumetric sampling and ratio of wind speed to sampling ratio.

4.4 Discussion

4.4.1 Inapplicability of existing theory

As shown in the results, the ratio of the sampling efficiency of the gravitational sampler to that of the volumetric sampler is proportional to the increase in wind speed, which means that the conventional conversion method is not able to calculate the volumetric pollen concentration from pollen deposition data because of the influence of wind speed. These results show that in some cases, inaccurate conversion between the gravitational sampler and the volumetric sampler is made either because the volumetric sampling efficiency decreases accompanied with the increase in wind speed or because the gravitational sampling efficiency increases accompanied with increase in wind speed.

4.4.2 Inadequacy of existing correction theory for volumetric sampler

The sampling efficiency is inherently independent of wind speed, which is widely assumed in discussions of sampling efficiency. This is derived from the following equations. From the continuity equation for particles, Eq. (36) holds:

$$C_0AV = C_Sav \tag{36}$$

where C_0 is the actual airborne pollen concentration, A is the cross-sectional area of the limiting trajectory, V is wind speed, C_S is the evaluated airborne pollen concentration, a is the cross-sectional area of the sampling tube, and v is the sampling rate. Additionally, from the continuity equation of air,

$$AV = av \tag{37}$$

Thus, from Eq. (36) and Eq. (37), the following result is derived, which is assumed to be true for any type of airborne particle sampling:

$$C_0 = C_S \tag{38}$$

However, previous studies suggest that the relationship between the sampled airborne particle concentration and the actual airborne particle concentration is a function of wind speed. Thus, to correct for the influence of wind speed on the sampling efficiency of volumetric samplers, a correction theory was introduced by Davies (1968) and improved by Vincent (2007). In the Davies theory, changes in the relative wind speed of ambient air to the sampling ratio proportionally influence changes in sampling efficiency because the changes in the inertial force have an effect on the particles, which is calculated as follows:

$$\alpha = 1 + \beta(R - 1) \tag{39}$$

$$\beta = 1 - \left\{\frac{1}{1 - 0.6Stln(1 - \frac{\delta}{2})}\right\} \tag{40}$$

where$\alpha$is the sampling efficiency, $R = v/V$, St is the Stokes' number, and δ is the diameter of the sampling tube.

These theories (Eq. (39) and Eq. (40)) explain that there is a possibility of a particle inside the limiting trajectory being pushed out of the limiting trajectory when the ambient wind speed is faster than the sampling rate. On the other hand, when the sampling rate is faster than the ambient wind speed, there is a chance of a particle outside the limiting trajectory irrupting over the limiting trajectory. a in Eq. (39) shows the theoretical probability of these crossovers occurring. Davies's theory has been significantly enhanced and used by various researchers. However, the results from the present study show a reverse trend in which an increase in wind speed causes an increase in the evaluated airborne pollen concentration. Thus, it is reasonable to say that additional influential factors resulted in the linear relationship between wind speed and the ratio of the sampling efficiency of the gravitational method to that of the volumetric method.

4.4.3 Introduction of new correction theory for gravitational samplers in turbulence

As discussed above, existing correction theory for volumetric sampler is not able to reflect the experimental results. Thus, introduction of a correction equation for theory to calculate the airborne pollen concentration from pollen deposition data (Eq. (34) and Eq. (35)), which has not been discussed yet, is required.

Because the conventional conversion theory for gravitational samplers was established under an assumption that the laminar flow is dominant, the conventional method might be no longer applicable when the turbulence is the dominant airflow at the sampling site. The dominant flow state, the laminar flow or the turbulent flow, at the experimental site is determined by the Reynolds number. The Reynolds number for the sampling condition in this experiment is calculated as Eq. (41) by substituting 4.2 m s^{-1}, the average wind speed for the duration of the experiment, for the wind speed and 3.0×10^{-1} m, the diameter of the laminas of the Durham sampler (d) for the characteristic length.

$$\begin{aligned} Re &= \frac{\rho V d}{\eta} \\ &= \frac{1.25 \times 4.2 \times 3.0 \times 10^{-1}}{1.5 \times 10^{-5}} \\ &\approx 1.05 \times 10^{5} \end{aligned} \tag{41}$$

Considering the fact that the Reynolds number is much larger than the laminar flow regime, the dominant flow at the sampling site was turbulent for the duration of sampling. Thus, it is reasonable to say that because the theoretical airborne pollen concentrations were calculated from the pollen deposition data using Eq. (34) and Eq. (35) under the assumption that the laminar flow is dominant, there are discrepancies between theoretically calculated airborne pollen concentrations and actual pollen concentrations at the experimental site at which the turbulent is dominant.

4.4.4 Reflecting turbulence influence to gravitational pollen sampling

As mentioned above, our results show that the existing calculation method is not applicable in turbulent though the conversion method of pollen deposition data to airborne pollen concentration in turbulent has never been considered.

The most characteristic difference between the laminar flow and the turbulent flow is that the flowlines in turbulent vibrate while the flowlines in the laminar flow are kept in a steady state.

Because the sampling plate is set between the two laminas, wind speed at each height in the Durham sampler is given as:

$$V = \frac{V_*}{\kappa} ln \frac{z}{Z_0} \tag{42}$$

where V_* is the friction velocity, κ is the Karman constant, Z_0 is the aerodynamic roughness, and z is the height from the bottom lamina in this experiment. This equation gives Eq. (43).

$$V_* = \kappa \left(ln \frac{z}{Z_0} \right)^{-1} V \tag{43}$$

For the particle diffusion caused by the turbulence, the diffusion coefficient is expressed as:

$$K = \frac{\kappa z}{\varphi} V_* \tag{44}$$

where φ is a coefficient.

By substituting Eq. (43) to Eq. (44), Eq. (45) is derived.

$$K = \frac{\kappa z}{\varphi} V_* = \frac{\kappa^2 z}{\varphi}\left(ln\frac{z}{Z_0}\right)^{-1} V \tag{45}$$

Therefore, the dispersion coefficient is proportional to wind speed at each height level.

$$K = \frac{\kappa^2 z}{\varphi}\left(ln\frac{z}{Z_0}\right)^{-1} V = const.V \tag{46}$$

Thus, accompanied with the increase in V, K also increases showing that the increase in wind speed promotes the vertical particle motion in the turbulence.

The vertical particle flux F is derived as follows by introducing the assumption used in the Inferential method for aerosol dry deposition:

$$F = K\frac{dc}{dz} \approx K\frac{C_0}{z} \tag{47}$$

Thus, the relationship between the number of sampled pollen grains and the actual airborne pollen concentration is expressed as:

$$N = \gamma Ft = \gamma const.V\frac{C_0}{z}t = const.' VtC_0 \tag{48}$$

where γ is a coefficient. As a result, because the amount of pollen deposition on the pollen sampling plate increases accompanied with an increase in wind speed as shown above, the airborne pollen concentration should be calculated using eq. (49), which is deformed from eq. (48).

$$C_0 = \frac{1}{const.'}\frac{N}{Vt} \tag{49}$$

With the assumption that the Hirst sampler shows the actual airborne pollen concentration, our experimental results actually show that the airborne pollen concentration is proportional to the ratio of the number of deposited pollen grains to wind speed (**Fig. 4.4**) when the average hourly airborne pollen concentration (C_V) is substituted to C_0 and the daily number of pollen grain sampled by the Durham sampler is substituted to N in eq. (49). Also, the slope of the relationship mentioned above is actually approximately constant (0.039 (2013); 0.031 (2014); 0.045 (2015); 0.047 (2016)). These results give the average value of $const.'$ as:

$$const.' \approx 24.7 \tag{50}$$

Although the value of $const.'$ was derived from our experimental results, more data are required to empirically determine the adequate value for $const.'$ as a future work.

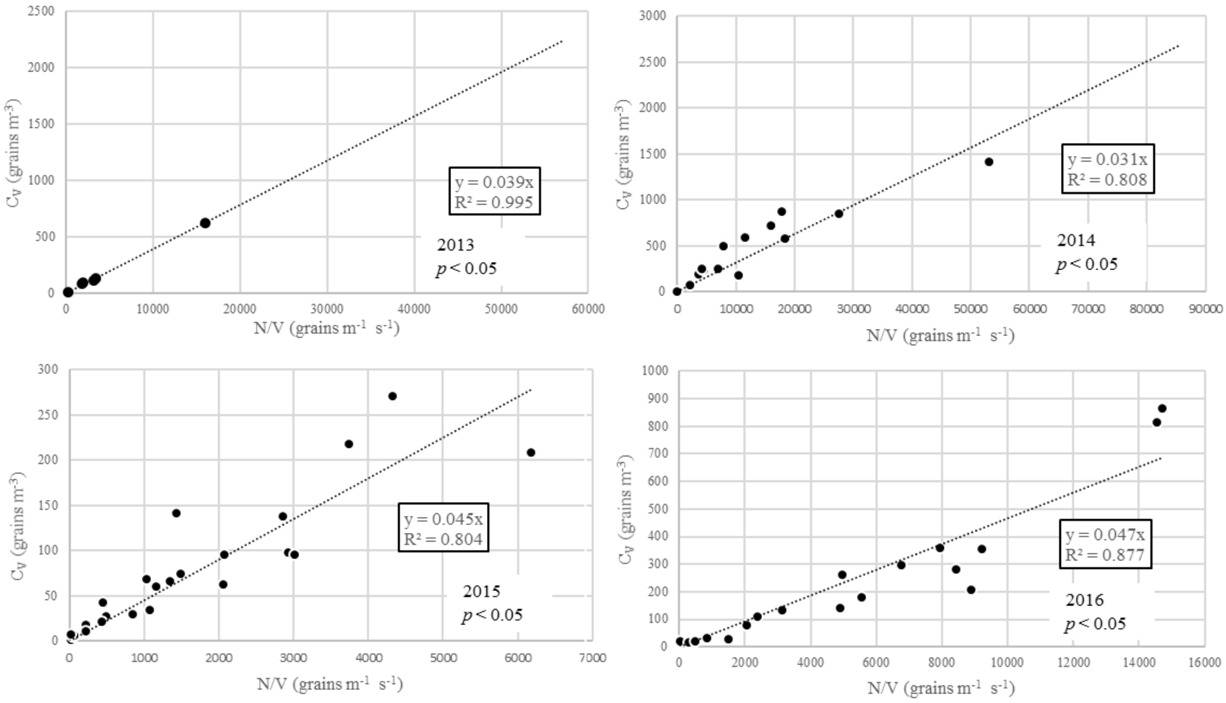

Fig. 4.4 Relationship between actual airborne pollen concentration (C_V) and ratio of number of pollen grains sampled using volumetric sampling method (N) to wind speed (V).

4.5 Conclusion

Our experimental results indicate that an existing and commonly used correction theory does not adequately explain the relationship between gravitational sampling and volumetric sampling because of the influence of wind speed. However, our newly proposed theory is able to explain the effect of wind speed by taking into consideration the fluctuation of vertical wind flux caused by turbulence. These results suggest that a drastic correction is required for the determination of airborne concentration of bioaerosols represented by pollen based on the data from the existing gravitational sampling methods.

Chapter 5

General conclusion

In this paper, the influence that the bioaerosol (pollen) transport condition and device-scale wind field have on pollen sampling efficiency has been analyzed via three comparisons. These comparisons were between 1. the Hirst-style sampling inlet and conical inlet, 2. the Hirst-style inlet and two-layered sampling inlet, and 3. the Hirst sampler and the Durham sampler.

In Chapter 1, previous aerobiological research was introduced to illustrate that sampling efficiency has not been fully analyzed from the viewpoints of aerodynamics and aerosol physics. In Chapter 2, the importance of wind speed and wind direction in determining the sampling efficiency is explained. It is also shown that the sampling efficiency is sensitively influenced by the device-scale wind field. Chapter 3 details how the sampling probability depends on the pollen grain size. This is due to the differences in the inertial force caused by variation in the pollen grains size resulting in changes to the probability of impaction. Chapter 4 focuses on the influence that the frequency of turbulence has on pollen deposition data. This is a factor that had not previously been given adequate consideration in the field of bioaerosol sampling.

The results of this research indicated the influence of the device-scale wind on the sampling efficiency. Moreover, the results imply that choosing an adequate set-up environment for the sampling device is of significant importance for accurate airborne bioaerosol concentration evaluation.

The Hirst sampler has been used widely, especially in Europe, as the reference for airborne pollen concentration determination. In this paper, various sampling methods (the conical inlet (Chapter. 2), the two-layered inlet (Chapter. 3), and the Durham sampler (Chapter. 4)) were compared with the Hirst-style sampler. The research presented in this paper suggests that the physical properties of non-Hirst style samplers influence the pollen sampling efficiencies of the instruments. In this context, the Hirst sampler was also applied effectively as a reference within this research. However, although Hirst-style samplers were used as a research reference in this paper, previous work had showed that, when particles are sampled from upwind, these particles are influenced by the inertial force caused by the relationship between the particle speed, wind speed and the sampling rate - as shown in Chapter 4. It is still not possible to make a definitive statement that the Hirst sampler accurately provides the actual airborne particle concentration. Additionally, when the airborne particle deposition and airborne particle motion in an airflow in device-scale has been analyzed from a Lagrangian point of view, a simplified wind field has been considered, in which the airflow is laminar. As a result, although the influence that turbulence has on the pollen deposition is discussed in Chapter 4, further research is required in order to comprehensively understand the relationship between turbulence and the bioaerosol sampling efficiency.

In conclusion, the relationship between the pollen sampling efficiency, with pollen being a representative bioaerosol, and the device-scale wind from an aerosol physics point of view has been analyzed. This has not been fully studied in previous works. Regarding future studies, the following two topics require investigation: 1. Analysis of the relationship between turbulent bioaerosol particle motion and the volumetric sampling efficiency 2. Determination of the actual sampling efficiency of the Hirst sampler based on further comparison with other varieties of sampler.

Acknowledgement

I would like to show my deep appreciation to my supervisors, honorary Professor Dr. Shigeto Kawashima and Professor Dr. Kimihito Nakamura at Kyoto University Graduate School of Agriculture for the patient guidance, encouragement and advice throughout my Masters and PhD student life.

I am grateful thanks to Professor Dr. Satoshi Hoshino and Professor Dr. Masayuki Fujihara, Kyoto University Graduate School of Agriculture, for becoming the member of the examination committee.

I also would like to express my gratitude for my other supervisor for manned space science, Professor Dr. Takao Doi at Kyoto University Unit of Synergetic Studies for Space, a former astronaut, for the guidance and advice from the planetary-scale aspect.

Dr. Bernard Clot at the Switzerland Federal Office of Meteorology and Climatology, Dr. Michael Thibaudon, at Le Réseau National de Surveillance Aérobiologique, and Mr. Toshio Fujita at Yamatoronics also made enormous contributions to the data acquisition and aerobiological analysis for this paper.

I would like to thank the members of the Hydrological Environment Engineering laboratory, especially to my lab fellow, Yi-Ting Tseng for sharing time and encouraging one another.

I also would like to show appreciation to Professor Dr. Satoshi Maeda at Hokkaido University, Dr. Miho Hatanaka at Nara institute of Science and Technology, and the late Dr. Keiji Morokuma, a former senior fellow at Kyoto University Fukui Institute for Fundamental Chemistry, for providing me with the first step to become a scientist.

Additional appreciation for Samuel J. Allen, a professional localizer, for his constructive advice and friendship.

Finally, I would like to express my appreciation to my family for all the support.

This work was supported by JSPS KAKENHI [grant number 201812315].

References

Adhikari, A., Martuzevičius, D., Reponen, T., Grishpun, S.A., Cho, S-H., Sivasubramani, S.K., Zhong, W., Levin, L.L., Kelly, A.L., St. Clair, H.G., Lemasters, G.K., 2003. Performance of the Button Personal Inhalable Sampler for the measurement of outdoor aeroallergens. *Atmos. Environ.* 37, 4723–4733.

Alcázar, P., Comtois, P., 2000. The influence of sampler height and orientation on airborne Ambrosia pollen counts in Montreal. *Grana* 39, 303–307. doi:10.1080/00173130052504342.

Aylor, D.E., 1998. The aerobiology of apple scab. *Pant Dis.* 82, 838–849. doi: 10.1094/PDIS.1998.82.8.838.

Ballach, J., Greuter, B., Schultz, E., Jaeschke, W., 1999. Variations of uptake rates in benzene diffusive sampling as a function of ambient conditions. *Sci. Total Environ.* 243–244, 203–217. doi:10.1016/S0048-9697(99)00387-3.

Bhat, M.M., Rajasab A.H., 1989. Efficiency of vertical cylinder spore trap and seven day volumetric Burkard spore trap in monitoring airborne pollen and fungal spores. *Grana* 28, 147–153. doi:10.1080/00173138909429966.

Blanco, C., de los Santos B., Barrau C., Arroyo F.T., Porras M., Romero F., 2004. Relationship among concentrations of *Sphaerotheca macularis* conidia in the air, environmental conditions and the incidence of powdery mildew in strawberry. *Plant Dis.* 88, 878－881. doi:10.1094/PDIS.2004.88.8.878

Brennan, G., L., Potter, C., de Vere, N., Griffith, G.W., Skjoth, C.A., Osborne N.J., Wheeler, B.W., McInnes, R.N., Clerlow, Y., Barber, A., Hanlon, H.M., Hegarty, M., Jones, L., Kurgansky, A., Rowney, F.M., Armitage, C., Adams-Groom, B., Ford, C.R., Petch, G.M., The PollerGEN Consortium, Creer, S., 2019. Temperate airborne grass pollen defined by spatio-temporal shifts in community composition. *Nat. Ecol. Evol.* 3, 750－754.

Bricchi, E., Frenguelli, G., Mincigrucci, G., 2000. Experimental results about *Platanus* pollen deposition. *Aerobiologia* 16, 347–352. doi:10.1023/A:1026701028901.

Brixey, L.A., Evans, D.E., Vincent, J.H., 2005. Aspiration efficiency of a thin-walled probe at right angles to the wind. *J. Aerosol Sci.* 36, 1144–1156. doi:10.1016/j.jaerosci.2004.12.007.

Bryan, N.C., Christner, B.C., Guzik, T.G., Granger, D.J., Stewart, M.F., 2019. Abundance and survival of microbial aerosols in the troposphere and stratosphere. *ISME J.* doi:10.1038/s41396-019-0474-0.

Buters, J.T.M., Antunes, C., Galveias, A., Bergmann, K.C., Thibaudon, M., Galán, C., Schmidt-Weber, C., Oteros, J., 2018. Pollen and spore monitoring in the world. *Clin. Transl. Allergy* 8, 9–13. doi:10.1186/s13601-018-0197-8.

Camacho, I.C., Caeiro, E., Ferro, R., Camacho, R., Camara, R., Grinn-Gofron, A., Smith, M., Strzelczak, A., Nunes, C., Morais-Almeida, M., 2017. Spatial and temporal variation in the annual pollen index recorded by sites belonging to the Portuguese Aerobiology Network. *Aerobiologia* 33, 265－279. doi: 10.1007/s10453-016-9468-9.

Carinanos, P., Sanchez-Mesa, J.A., Prieto-Baena, J.C., Lopez, A., Guerra, F., Moreno, C., 2002. Pollen allergy related to the area of residence in the city of Cordoba, south-west Spain. *J. Environ. Monit*. 4, 734－738. doi: 10.1039/b205595c.

Carvalho, E., Sindt, C., Verdier, A., Galan, C., O'Donoghue, L., Parks, S., Thibaudon, M., 2008. Performance of the Coriolis air sampler, a high-volume aerosol-collection system for quantification of airborne spores and pollen grains. *Aerobiologia* 24, 191–201. doi:10.1007/s10453-008-9098-y.

Cocke, E.C., 1937. Calculating pollen concentration of the air. *J. Allergy Clin. Immunol*. 8, 601－606.

Cornell, R.C., Welch, S.F., Hall, L.B., 1961. A comparison of gravimetric and volumetric pollen samplers. *J. Allergy* 32, 128–134.

Crisp, H.C., Gomez, R.A., White, K.M., Quinn, J.M., 2013. A side-by-side comparison of Rotorod and Burkard pollen and spore collections. *Ann. Allergy Asthma Immunol.* 111, 118–125. doi:10.1016/j.anai.2013.05.021.

Crispen, K.L., Gillespie, D.N., Weiler, E.C., Noonan, C.W., Hamilton, R.F., Ward, T.J., 2010. A comparison of 1978 and 2006 peak pollen seasons and sampling methods in Missoula, Montana. *Grana* 49, 128–133. doi:10.1080/00173131003587049.

Crouzy, B., Stella, M., Konzelmann, T., Calpini, B., Clot, B., 2016. All-optical automatic pollen identification: Towards an operational system. *Atmos. Environ.* 140, 202–212. doi:10.1016/j.atmosenv.2016.05.062.

Davies, C. N., 1968. The entry of aerosol into sampling tubes and heads. *J. Physics D: Applied Physics* 1, 921–932.

Delaunay, J.J., Sasajima, H., Okamoto, Y., Yokota, M., 2007. Side-by side comparison of automatic pollen counters for use in pollen information systems. *Ann. Allergy Asthma Immunol.* 98, 553–558.

Deptula, M., Filbrandt-Czaja, A., Nienartowicz, A., Kaminski, D., Adamska, E., Piernik, A., Lewandowska-Czarnecka, A., 2018. Development of forests in the former heathland landscape: changes in the habitat quality, structure of undergrowth, syntaxonomy of phytocoenoses and modern pollen deposition. *Ecological questions* 29, 19–40. doi: 10.12775/EQ.2018.016.

Erkan, P., Bicakci, A., Aybeke, M., Malyer, H., 2011. Analysis of airborne pollen grains in Kirklareli. *Turk. J. Bot.* 35, 57－65. doi:10.3906/bot-0903-1.

Erkara, I.P., Cingi, C., Ayranci, U., Gurbuz, K.M., Pehlivan, S., Tokur, S., 2009. Skin prick test reactivity in allergic rhinitis patients to airborne pollens. *Environ. Monit. and Assess.* 2151, 1－4. doi: 10.1007/s10661-008-0284-8.

Estrella, N. Menzel, A., Kr ämer, U., Behrendt, H., 2006. Integration of flowering dates in phenology and pollen counts in aerobiology: analysis of their spatial and temporal coherence in Germany (1992-1999). *Int. J. Biometeorol.* 51, 49 – 55. doi:10.1007/s00484-006-0038-7.

Ezike, D.N., Nnamani, C.V., Ogundipe, O.T. Adekanmbi, O.H., 2016. Airborne pollen and fungal spores in Garki, Abuja (North-Central Nigeria). *Aerobiologia* 32, 697–707. doi 10.1007/s10453-016-9443-5.

Fan, B., McFarland, A.R., Anand, N.K., 1992. Aerosol particle losses in isokinetic sampling probe inlets. *Environ. Sci. Technol.* 26, 390–394. doi:10.1021/es00026a022.

Favero-Longo S.E., Sandrone, S., Matteucci, E., Appolonia, L., Piervittori, R., 2014. Spores of lichen-forming fungi in the mycoaerosol and their relationships with climate factors. *Sci. Total Environ.* 466–467, 26–33. doi:10.1016/j.scitotenv.2013.06.057.

Feinberg, S.M., Steinberg, M.J., 1933. Studies in pollen potency. *J. Allergy* 5, 19 – 28. https://doi.org/10.1016/S0021-8707(33)90166-5.

Fernández-Llamanzares, Á., Belmonte, J., Boada, M., Fraixedas, S., 2014. Airborne pollen records and their potential applications to the conservation of biodiversity. *Aerobiologia* 30, 111-122. doi:10.1007/s10453-013-9320-4.

Fernández-Rodríguez, S., Skjoth, C.A., Tormo-Monila R., Brandao, R. Caeiro, E. Silva-Palacios, I., Gonzalo-Garijo, Á, Smith, M., 2014. Identification of potential sources of airborne *Olea* pollen in the Southwest Iberian Peninsula. *Int. J. Biometeorol.* 58, 337-348. doi: 10.1007/s00484-012-0629-4.

Fernandez, M.O., Thomas, R.J., Garton, N.J., Hudson, A., Haddrell, A., Reid, J.P., 2019. Assessing the airborne survival of bacteria in populations of aerosol droplets with a novel technology. *J. Royal Soc. Interface.* 16. doi:10.1098/rsif.2018.0779.

Fiorina, A., Scordamaglia, A., Mincarini, M., Fregonese, L., Canonica, G.W., 1997. Aerobiologic particle sampling by a new personal collector (Partrap FA52) in comparison to the Hirst (Burkard) sampler. *Allergy* 52, 1026–1030. doi:10.1111/j.1398-9995.1997.tb02426.x.

Frenz, D. A., 1999. Comparing pollen and spore counts collected with the Rotorod sampler and Burkard spore trap. *Ann. Alergy Asthma Immunol.* 83, 341–347.

Frenz, D. A., 2001. Interpreting atmospheric pollen counts for use in clinical allergy: allergic symptomology. *Ann. Alergy Asthma Immunol*. 86, 150–157.

Frinking H.D., 1991. Aerobiology of "closed" agricultural systems. *Grana* 30, 481－485.

Gagnon, L., Comtois, P., 1992. Are sampling results from different pollen traps comparable? *Grana* 31, 125–130.

Galan, C., Alcazar, P., Carinanos, P., Garcia, H., Dominguez-Vilches, E., 2000. Meteorological factors affecting daily Urticaceae pollen counts in southwest Spain. *Int. J. Biometeorol.* 43,191–195.

Galeev, R.S., Zaripov, S.K., 2003. A theoretical study of aerosol sampling by an idealized spherical sampler in calm air. *J. Aerosol Sci*. 34, 1135–1150. doi:10.1016/S0021-8502(03)00091-0.

García-Mozo, H., Oteros, J.A., Galán, C., 2016. Impact of land cover changes and climate on the amin airborne pollen types in Southern Spain. *Sci. Total Environ.* 548, 221－228. doi:10.1016/j.scitotenv.2016.01.005.

Giesecke, T., Fontana, S.L., van der Knaap, W.O., Pardoe, H.S., Pidek, I.A., 2010. From early pollen trapping experiments to the Pollen Monitoring Programme. *Veg. Hist. Archaeobot.* 19, 247–258. doi: 10.1007/s00334-010-0261-3.

Gioulekas, D., Balafoutis, C., Damialis, A., Papakosta, D., Gioulekas, G., Patakas, D., 2004. Fifteen year's record of airborne allergenic pollen and meteorological parameters in Thessaloniki, Greece. *Int. J. Biometeorol*. 48, 128–136.

Gomez-Domenech, M., Garcia-Mozo, H., Alcazar, P., Brandao, R., Caeiro, E., Munhoz, V., Galan, C., 2010. Evaluation of the efficiency of the Coriolis air sampler for pollen detection in South Europe. *Aerobiologia* 26, 149-155. doi:10.1007/s10453-009-9152-4.

Grinshpun, S.A., Chang, C.W., Nevalainen, A., Willeke, K., 1994. Inlet characteristics of bioaerosol samplers. *J. Aerosol Sci*. 25, 1503–1522. doi:10.1016/0021-8502(94)90221-6.

Gupta, A., Stathopoulos, T., Saathoff, P., 2012. Wind tunnel investigation of the downwash effect of a rooftop structure on plume dispersion. *Atmos. Environ.* 46, 496–507.

Hamada, T., Terry, L. I., Marler, T. E., 2015. Habitats, trade winds, and pollination of the endangered ycas Micronesica: Is there a role for wind as pollen vector on the Island of Guam? *Int. J. Plant Sci*. 176, 525–543.

Hangal, S., Willeke, K., 1990. Overall efficiency of tubular inlets sampling at 0–90 degrees from horizontal aerosol flows. *Atmos. Environ*. Part A. General Topics 24, 2379–2386. doi:10.1016/0960-1686(90)90330-P.

Hartill W.F.T., 1980. Aerobiology of *Sclerotinia sclerotiorum* and *Botrytis cinerea* spores in New Zealand tobacco crops. *New Zeal. J. Agr. Res.* 23, 259 – 262. doi:10.1080/00288233.1980.10430796.

Hassan, M.S., Lau, R., 2011. Inhalation performance of pollen-shape carrier in dry powder formulation: Effect of size and surface morphology. *Int. J. Phar.* 413, 1 – 2. doi:10.1016/j.ijpharm.2011.04.033.

Heffer, M.J., Ratz, J.D., Miller, J.D., Day, J.H., 2005. Comparison of the Rotorod to other air samplers for the determination of *Ambrosia artemisiifolia* pollen concentrations conducted in the Environmental Exposure Unit. *Aerobiologia* 21, 233–239. doi:10.1007/s10453-005-9007-6

Hinds, W.C., 1999. Bioaerosols, in: Aerosol Technology 2nd Edn. John Wiley & Sons, New York, pp. 394–400.

Hofmann, F., Kruse-Plass, M., Kuhn, U., Otto, M., Schlechtriemen, U., Schröder, B., Vögel, R., Wosniok, W., 2016. Accumulation and variability of maize pollen deposition on leaves of European Lepidoptera host plants and relation to release rates and deposition determined by standardized technical sampling. *Environ. Sci. Europe*, 28. doi: 10.1186/s12302-016-0082-9.

Hrga, I., Mitic, B., Alegro, A., Dragojlovic, D., Stjepanovic, B., Puntaric, D., 2010. Aerobiology of sweet chestnut (*Castanea sativa* Mill.) in north-west Croatia. *Coll. Antropol*. 34, 501 – 507.

Hussain, M.M., Mandal, J., Bharracharya, K., 2014. Aerobiological, clinical, and immunobiochemical studies on *Alstonia scholaris* pollen from eastern India. *Environ. Moni. Assess*. 186, 457–467. doi:10.1007/s10661-013-3390-1.

Immler, F., Engelart, D., Schremes, O., 2005. Fluorescence from atmospheric aerosol detecte by a lidar indicates biogenic particles in the lowermost stratosphere. *Atmos. Chem. Phys*. 5, 345–355. doi: 10.5194/acp-5-345-2005.

Jarosz, N., Loubet, B., Durand B., Mccartney, A., Foueillassar, X., Huber, L., 2003. Field measurements of airborne concentration and deposition rate of maize pollen. *Agric. For. Meteorol*. 119, 37–51. doi:10.1016/S0168-1923(03)00118-7.

Jedryczka, M., Strzelczak, A., Grinn-Gofron, A., Nowak, M., Wolski, T., Siwulski, M., Sobieralski, K., Kaczmarek, J., 2015. Advanced statistical models commonly applied in aerobiology cannot accurately predict the exposure of people to *Ganoderma* spore-related allergies. *Agric. For. Meteorol*. 201, 209–217. doi:10.1016/j.agrformet.2014.11.015.

Jochner, S., Ziello, C., Bo¨ck, A., Estrella, N., Buters, J., Weichenmeier, I., Behrendt, H., Menzel, A., 2012. Spatio-temporal investigation of flowering dates and pollen counts in the topographically complex Zugspitze area on the German-Austrian border. *Aerobiologia*, 28, 541–556. doi:10.1007/s10453-012-9255-1.

Kasprzyk, I., Ortyl, B., Dulska-Jez, A., 2014. Relationships among weather parameters, airborne pollen and seed crops of Fagus and Quercus in Poland. *Agr. and Forest Meteorol*. 197, 111–122.

Kawashima, S., Clot, B., Fujita, T., Takahashi, Y., Nakamura, K., 2007. An algorithm and a device for counting airborne pollen automatically using laser optics. *Atmos. Environ.* 41, 7987–7993. doi:10.1016/j.atmosenv.2007.09.019.

Kawashima, S., Thibaudon, M., Matsuda, S., Fujita, T., Lemonis, N., Clot, B., Oliver, G., 2017. Automated pollen monitoring system using laser optics for observing seasonal changes in the concentration of total airborne pollen. *Aerobiologia* 33, 351–362. doi:10.1007/s10453-017-9474-6.

King, M.F., Noakes, C.J., Sleigh, P.A., Camargo-Valero, M.A., 2013. Bioaerosol deposition in single and two-bed hospital rooms: A numerical and experimental study. *Build. Environ.* 59, 436–447. doi:10.1016/j.buildenv.2012.09.011.

Kizilpinar, I., Civelek, E., Tuncer, A., Dogan, C., Karabulut, E., Sahiner, U. M., Yavuz, S. T., Sackesen, C., 2011. Pollen counts and their relationship to Meteorological factors in Ankara, Turkey During 2005-2008. *Int. J. Biometeorol*. 55, 623–631.

Kreissl, B., Höschele, K., Staiger, H., Schultz, E., 1991. Meteorological influence on particle dry deposition. *J. Aerosol Sci*.: Proceedings of the 1991 European Aerosol Conference 22, S573–S576. doi:10.1016/S0021-8502(05)80166-1.

Laaidi, K., 2001. Predicting days of high allergenic risk during *Betula* pollination using weather types. *Int. J. Biometeorol*. 45, 124–132. doi:10.1007/s004840100096.

Lackemeyer, M.G., de Kok-Mercado, F., Wada, J., Bollinger, L., Kindrachunk, J., Wahl-Jensen, V., Kuhn, J.H., Jahrling, P.B., 2014. ABSL-4 aerobiology biosafety and technology at the NIH/NIAID integrated research facility at fort detrick. *Viruses*. 6, 137–150. doi:10.3390/v6010137.

Latorre, F., Romero, E. J., Mancini, M. V., 2008. Comparative study of different methods for capturing airborne pollen, and effects of vegetation and meteorological variables. *Aerobiologia* 24, 107–120.

Levetin, E., Rogers, C. A., Hall, S. A., 2000. Comparison of pollen sampling with a Burkard spore trap and a Tauber trap in a warm temperature climate. *Grana* 39, 294–302.

Levin, L., M., 1957. The intake of aerosol samples, *Bulletin of the Academy of Sciences of the U.S.S.R. Geophysics* 7, 914–925. [in Russian]

Li, J., Li, Y.C., Zhang, Z., Li, Y., Wang, C.Y., 2018. The dispersion characteristics of airborne pollen in the Shijiazhuang (China) urban area and its relationship with meteorological factors. *Aerobiologia* 34, 89–104. doi: 10.1007/s10453-017-9501-7.

Li, S.-N., Lundgren, D.A., 2002. Aerosol aspiration efficiency of blunt and thin-walled samplers at different wind orientations. *Aerosol Sci. Tech*. 36, 342–350. doi:10.1080/027868202753504533.

Lu, S., Inoue, S., Shibaike, H., Kawashima, S., Yonemura, S., Du, M., 2015. Detection potential of maize pollen release stage by using vegetation indices and red edge obtained from canopy reflectance in visible and NIR region. *J. Agri. Meteorol*. 71, 153–160. doi:10.2480/agrmet.D-14-00035.

Masuda, H., Yoshida, H., 1974. The intake of aerosol samples - On the Levin's paper -, *Advanced Powder Technol*. 11, 333–338. [in Japanese]

Mavroidis I., Andronopoulos, S., Bartzis, J. G., Griffiths, R. F., 2007. Atmospheric dispersion in the presence of a three-dimensional cubical obstacle: modeling of mean concentration and concentration fluctuations. *Atmos. Environ.* 41, 2740–2756.

Mehta, S. K., Mishra, S. K., Pierson, D. L., 1996. Evaluation of three portable samplers for monitoring airborne fungi. *Appl. Environ. Microbiol*. 62, 1835–1838.

Michel, D., Rotach, M.W., Gehrig, R., Vogt, R., 2012. On the efficiency and correction of vertically oriented blunt bioaerosol samplers in moving air. *Int. J. Biometeorol*. 56, 1113-1121, doi:10.1007/s00484-012-0526-x.

Mitsumoto, K., Yabusaki, K., Kobayashi, K., Aoyagi, H., 2010. Development of a novel real-time pollen-sorting counter using species-specific pollen autofluorescence. *Aerobiologia* 26, 99–111.

Molina, R. T., Manzano, J. M., M., Rodríguez, S. F., Garijo, Á., G., Palacios, I. S., 2013. Influence of environmental factors on measurements with Hirst spore traps. *Grana* 52, 59–70.

Monroy-Colin, A., Silva-Palacios, I., Tormo-Molina, R., Maya-manzano, J.M., Rodoriguez, S.F., Gonzalo-Garijo, A.E., 2018. Environmental analysis of airborne pollen occurrence, pollen source distribution and phenology of *Fraxinus angustifolia*, *Aerobiologia* 34, 269－283. doi: 10.1007/s10453-018-9512-z.

Moreno-Grau, S., Bayo, J., Elvira-Rendueles, B., Angosto, J.M., Moreno, J.M., Moreno-Clavel, J., 1998. Statistical evaluation of three years of pollen sampling in Cartagena, Spain. Grana 37, 41－47. doi: 10.1080/00173139809362638.

Morris, C.E., Sands, D.C., Bardin, M., Jaenicke, R., Vogel, B., Leyronas, C., Ariya, P.A., Psenner, R., 2011. Microbiology and atmospheric processes: research challenges concerning the impact of airborne micro-organisms on the atmosphere and climate. *Biogeosciences* 8, 17–25. doi:10.5194/bg-8-17-2011.

Mullins, J., Emberlin, J., 1997. Sampling pollens. *J. Aerosol Sci.* 28, 365–370.

O’Conner, D.J., Healy, D.A., Sodeau, J.R., 2015. A 1-month onliune monitoring campaign of ambient fungal spore concentrations in the harbour region of Cork, Ireland. *Aerobiologia* 31, 295–314. doi:10.1007/s10453-015-9365-7.

Olmsted, R.N., 2008. Pilot study of directional airflow and containment of airborne particles in the size of *Mycobacterium tuberculosis* in an operating room. *Am. J. Infect. Control* 36, 260–267. doi:10.1016/j.ajic.2007.10.028.

Oteros, J., Sofiev, M., Smith, M, Clot, B., Damialis, A., Prank, M., Werchan, M., Wachter, R., Weber, A., Kutzura, S., Heinze, S., Herr, C.E.W., Menzel, A., Bergmann, K.C., Traidl-Hoffmann, C., Schmit-Weber, C.B., Buters, J.T.M., 2019. Building an automatic pollen monitoring network (ePIN): Selection of optimal sites by clustering pollen stations. *Sci. Total Environ*. 688, 1263–1274. doi:10.1007/s10453-014-9335-5.

Pawankar, R., Canonica, G. W., Holgate, S. T., Lockey, R. F., 2011. *World Allergy Organization (WAO)* White *Book on Allergy*. World Allergy Organization, 5.

Peel, R. G., Kennedy, R., Smith, M., Hertel, O., 2014. Relative efficiencies of the Burkard 7-day, Rotorod and Burkard Personal Samplers for Poaceae and Urticaceae pollen under field conditions. *Ann. Agr. Env. Med*. 21, 745–752.

Peternel, R., Čulig, J., Hrga, I., Hercog, P., 2006. Airborne ragweed (*Ambrosia artemisiifolia* L.) pollen concentrations in Croatia, 2002-2004. *Aerobiologia* 22, 161–168. doi:10.1007/s10453-006-9028-9.

Phillpotts, R.J., Thomas R.J., Beedham, R.J., Platt, S.D., Vale, C.A., 2010. The Cystovirus phil6 as a simulant for Venezuelan equine encephalitis virus. *Aerobiologia* 26, 301–309. doi:10.1007/s10453-010-9166-y.

Picco, A.M., Rodolfi, M., 2000. Airborne fungi as biocontaminants at two Milan underground stations. *Int. Biodeter. Biodegr.* 45, 43–47.

Prado, N., de Linares, C., Sanz, M.L., Gamboa, P., Villalba, M., Rodriguez, R., Batanero, E., 2015. Pollensomes as natural vehicles for pollen allergens. *J. Immunol.* 195, 445–449. doi:10.4049/jimmunol.1500452.

Riediker, M., Keller, S., Wüthrich, B., Koller, T., Monn, C., 2000. Personal pollen exposure compared to stationary measurements. *Invest. Allergol. Clin. Immunol*. 10, 200–203.

Riediker, M., Koller, T., Monn, C., 2000. Differences in size selective aerosol sampling for pollen allergen detection using high-volume cascade impactors. *Clin. Exp. Allergy* 30, 867–873. doi:10.1046/j.1365-2222.2000.00792.x.

Ríos B., Torres-Jardón R., Ramírez-Arriaga, E., Martínez-Bernal A., Rosas, I., 2016. Diurnal variations of airborne pollen concentration and the effect of ambient temperature in three sites of Mexico City. *Int. J. Biometeorol*. 60, 771–787. doi:10.1007/s00484-015-1061-3.

Ritenberga, O., Sofiev, M., Silijamo, P., Saarto A., Dahl, A., Ekebom, A., Sauliene, I., Shalaboda, V., Severova, E., Hoebeke, L., Ramfjord, H., 2018. A statistical model for predicting the inter-annual variability of birch pollen abundance in Northern and North-Eastern Europe. *Sci. Total Environ.* 615, 228–239. doi:10.1016/j.scitotenv.2017.09.061.

Rojo, J., Rapp, A., Lara, B., Fernández-González, F., Pérez-Badia, R., 2015. Effect of land uses and wind direction on the contribution of local sources to airborne pollen. *Sci. Total Environ.* 538, 672–682. doi:10.1016/j.scitotenv.2015.08.074.

Sadyś, M., 2017. Effects of wind speed and direction on monthly fluctuations of *Cladosporium* conidia concentration in the air. *Aerobiologia* 33, 445–456. doi:10.1007/s10453-017-9482-6.

Santos, J. M., Griffiths, R. F., Roberts, I. D., Reis, N. C., 2005. A field on turbulent concentration fluctuations of an atmospheric tracer gas in the vicinity of a complex-shaped building. *Atmos. Environ.* 39, 4999–5012.

Šauliene, I., Veriankaite, L., 2012. Analysis of high allergenicity airborne pollen dispersion: common ragweed study case in Lithuania. *Ann. Agr. Environ. Med.* 19, 415–419.

Šauliene, I., Šukiene, L., Daunys, G., Valiulis, G., Vaitkevicius, L., Matavulj, P., Brdar, S., Panic, M., Sikoparija, B., Clot, B., Crouzy, B., Sofiev, M., 2019. Automatic pollen recognition with the Rapid-E particle counter: the first-level procedure, experience and next steps. *Atmos.Meas.Tech.* 12, 3435－3452. doi:10.5194/amt-12-3435-2019.

Scheppegrell, W., 1917. Hay-fever and hay fever pollens. *Arch. Intern. Med*. 19, 959－980. doi: 10.1001/archinte.1917.00080260002001.

Serrano-Silva, N., Calderon-Ezquerro, M.C., 2018. Metagenomic survey of bacterial diversity in the atmosphere of Mexico City using different sampling methods. *Environ. Pollut.* 235, 20–29. doi:10.1016/j.envpol.2017.12.035.

Smith, D.J., Ravichandar, J.D., Jain, S., Griffin, D.W., Yu, H., Tan, Q., Thissen, J. Lusby, T., Nicoll, P., Shedler, S., Martinez, P., Osorio, A., Lechniak, J., Choi, S., Sabino, K., Iverson, K., Chan, L., Jaing, C., McGrath, J., 2018. Airborne bacteria in earth's lower stratosphere resemble taxa detected in the troposphere: Results from a new NASA Aircraft Bioaerosol Collector (ABC). *Front. Microbiol*. 14. doi: 10.3389/fmicb.2018.01752.

Sreenath, A., Ramachandran, G., Vincent, J. H., 2002. Aspiration characteristics of idealized blunt aerosol samplers at large angles to the wind. *J. Aerosol Sci*. 33, 871–881. doi:10.1016/S0021-8502(02)00041-1.

Su, W.C., Vincent, J.H., 2002. New experimental studies to directly measure aspiration efficiencies of aerosol samplers in calm air. *J. Aerosol Sci*. 33, 103–118. doi:10.1016/S0021-8502(01)00156-2.

Sun, L.Y., Xu Y.H., Wang, Y.W., Lou, Y.Y., Xu, Y.P., Guo, Y.S., 2017. Species and quantity of airborne pollens in Shanghai as monitored by gravitational and volumetric methods. *Asian Pac. J. Allergy* 35, 38–45. doi: 10.12932/AP0743.

Surbek, M., Esen, C., Schweiger, G., Ostendorf, A., 2011. Pollen Characterization and Identification by Elastically Scattered Light. *J. Biophotonics* 4, 49–56.

Takahashi, Y., Kawashima, S., Suzuki, Y., Ohta, N., Kakehata, S., 2018. Enrichment of airbotne Japanese cedar (*Cryptomeria japonica*) pollen in mountain ranges when passing through a front accompanying temperate low pressure. *Aerobiologia* 34, 105–110. doi:10.1007/s10453-017-9494-2.

Taylor,P.E., Flagan, R.C., Valenta, R., Glovsky, M.M., 2002. Release of allergens as respirable aerosols: A link between grass pollen and asthma. *J. Allergy Clin. Immunol*. 109, 51–56 doi:10.1067/mai.2002.120759.

Thibaudon, M., Oliver, G., Sindt, C., 2009. The pollen trap: A tool to determine the origin of ragweed pollens. *Revue Française d'Allergologie* 49, 515–523.

Thibaudon, M., Caillaud, D., Besancenot J. P., 2013. Methods of studying airborne pollen and pollen calendars. *Revue des Maladies Respiratoires* 30, 463–479.

Tomás, C., Candau, P., Gonzalez Minero, F.J., 1997. A comparative study of atmospheric pollen concentrations collected with Burkard and Cour samplers, Seville (Spain) 1992-1994. *Grana* 36, 122–128. doi:10.1080/00173139709362598

Tosunoğlu, *A.*, Yenıgün, A., Biçaçi Elıaçik, K., 2013. Airborne pollen content of Kuşadası. *Turkish J. Bot.* 37, 297－305. doi: 10.3906/bot-1203-5.

Toth, I., Peternel, R., Srnec, L., Vojnikovic, B., 2011. Diurnal variation in airborne pollen concentrations of the selected taxa in Zagreb, Croatia. Collegium *Antropologicum* 35, 43–50.

Velasco-Jiménez, M.J., Alcázar, P., Valenzuela, L.R., Gharbi, D., Díaz de la Guardia, C., Galán, C., 2017. Pinus pollen season trend in South Spain. *Plant biosyst*. 152, 657–665, doi: 10.1080/11263504.2017.1311962.

Veriankaite, L., Sauliene, I., Bukantis, A., 2011. Evaluation of meteorological parameters influence upon pollen spread in the atmosphere. *J. Environ. Eng. and Landsc*. 19, 5–11.

Vincent, J. H., 1987. Recent advances in aspiration theory for thin-walled and blunt aerosol sampling probes. *J. Aerosol Sci*. 18, 487–498.

Vincent, J.H., 2007. Aerosol aspiration in moving air, in; Aerosol sampling science, standards, instrumentation and applications. John Wiley & Sons, New York; pp. 93－130.

Visez, N., Chassard, G., Azarkan, N., Naas, O., Sénéchal, H., Sutra, J.-P., Poncet, P., Choël, M., 2015. Wind-induced mechanical rupture of birch pollen: Potential implications for allergen dispersal. *J. Aerosol Sci*. 89, 77–84. doi:10.1016/j.jaerosci.2015.07.005.

Volkova,O., Severova, E., 2017. A comparison of modern pollen rain collected by Hirst type and Tauber traps in Moscow, *Russia. ecological questions* 26, 15–17. doi:10.12775/EQ.2017.010.

Wen, X., Ingham, D.B., 2000. Aspiration efficiency of a thin-walled cylindrical aerosol sampler at yaw orientations with respect to the wind. *J. Aerosol Sci*. 31, 1355–1365. doi:10.1016/S0021-8502(00)00036-7.

West, J.S., Kimber, R.B.E., 2015. Innovations in air sampling to detect plant pathogens. *Ann. Appl. Biol*. 166, 4–17. doi:10.1111/aab.12191.

Willeke, K., Grinshpun, S. A., Chang, C. W., Juozaitis, A., Liebhaber, F., Nevalainen, A., Thompson, M., 1992. Inlet sampling efficiency of bioaerosol samplers. *J. Aerosol Sci*. 23, 652–654.

Yamamoto, N., Matsuki, H., Yanagisawa, Y., 2007. Application of the personal aeroallergen sampler to assess personal exposure to Japanese cedar and cypres pollens. *J. Expo. Sci. Environ. Epidemiol.* 17, 637–643. doi: 10.1038/sj.jes.7500549.

Yamamoto, N., Nishikawa, J., Sakamoto, M., Shimizu, T., Matsuki, H., 2010. Indoor and Outdoor Concentration of Japanese Cedar Pollens and Total Suspended Particulates: A Case Study at a Kindergarten in Japan. *Build. Environ.* 45, 792–797.

Yasaka, M., Kobayashi, S., Yakeuchi, S., Tokuda, S., Takiya, M., Ohno, Y., 2009. Prediction of birch airborne pollen counts by examining male catkin numbers in Hokkaido, northern Japan. *Aerobiologia* 25, 111-117. doi:10.1007/s10453-009-9116-8.

Yli-Panula, E., Fekedulegn, D.B., Green, B.J., Ranta, H. 2009. Analysis of airborne *Betula* pollen in Finland; a 31-year perspective. *Int. J. Environ. Res. Public Health* 6, 1706–1723. doi:10.3390/ijerph6061706.

Zhang, R., Duhl, T., Salam, M.T., House, J.M., Flagan, R.C., Avol, E.L., Gilliland, F.D., Guenther, A., Chung, S.H., Lamb, B.K., VanReken, T.M., 2014. Development of a regional-scale pollen emission and transport modeling framework for investigating the impact of climate change on allergic airway disease. *Biogeosciences* 11, 1461–1478. doi:10.5194/bg-11-1461-2014.